8825 p-52

ds ØM 593208 [illegible]

OSU

The Ohio State University

SIMULATION OF AN AIRCRAFT FLYING THROUGH
A GROUND STATION TO SATELLITE LINK

by

R.C. Rudduck
W.D. Burnside
A.K. Dominek
T.H. Lee

The Ohio State University

**ElectroScience Laboratory**

Department of Electrical Engineering
Columbus, Ohio 43212

(NASA-CR-176845) SIMULATION OF AN AIRCRAFT FLYING THROUGH A GROUND STATION TO SATELLITE LINK (Ohio State Univ.) 52 p HC A04/MF A01 CSCL 20N N86-26487

Unclas
G3/32 43428

Technical Report 716148-7
Grant No. NSG 1613
February 1986

National Aeronautics and Space Administration
Langley Research Center
Hampton, Virginia 23665

# NOTICES

TABLE OF CONTENTS

## LIST OF TABLES

LIST OF FIGURES

| Figure | | Page |
|---|---|---|

# I. INTRODUCTION

The potential for an aircraft to fly directly through a ground station-to-satellite link becomes more significant if the link is located closer to an airport, obviously. Because this situation is much more likely near airports, it is appropriate to examine the effects of such an encounter.

There are two aspects to the work reported here: (1) an aperture blockage theoretical solution developed by Rudduck and Lee [1] was used to calculate the effect of a large aircraft (C5) for various satellite ground station antenna diameters, and (2) the compact range facility at the Ohio State University was used to measure various targets, including a 737 aircraft, and to validate the theoretical solution in item (1).

## II. SCALE MODEL MEASUREMENTS

In order to simulate this problem, the compact range at The Ohio State University was used to simulate the satellite antenna; whereas, a three foot diameter dish was used in the back of the anechoic chamber to model the ground station receiver. A 14-1/2 foot long linear prober was then placed on the chamber floor just behind the compact range feed and oriented orthogonal to the line from the compact range reflector to the three foot dish in the back of the room. This configuration is illustrated in Figure 1*. A styrofoam pedestal was then placed on the linear prober which was used to hold various targets that could be drawn through the simulated line-of-sight link. Some example targets used for this study are shown in Figure 2 being drawn across the room. The system was constructed to operate at Ku-band so that any frequency from 12 to 18 GHz could be used. The target was positioned 28 feet from the simulated ground station antenna such that if a 60 foot dish were being scale modelled with this system, the simulated full scale frequency would be 400 to 600 MHz at a range of 840 feet. Note that these results could be scaled by other factors to simulate other situations. In addition, the measured results have also been used to validate the aperture blockage theoretical solution developed by Rudduck and Lee [1] which can be used to simulate any potential problem.

It was our feeling from the onset that the major problem associated with an aircraft flying through such a link would be related to the

*Note: For the convenience of the reader, all figures and tables have been grouped together at the end of the report.

forward scattering of the aircraft. It has been known for many years that forward scattering is simply related to the cross-sectional shape of the target which blocks the direct signal. In other words, the aircraft forward scattering can be simulated by a flat plate whose cross-section models the blockage cross-section of the aircraft. One can think of the satellite as a flashlight which is pointed toward a wall. Then place an object between the light and the wall. One will observe that the image seen on the wall is representative of the cross-sectional structure blocking the light path. Our simulated measured results were then used to see if our forward scattering model was correct for this type of problem. To show this, various geometries were measured along with equivalent flat plates used to simulate the blockage cross-section. Some of these targets are shown in Figure 3.

The complete set of measured data will be presented in a future report; however, a few examples are shown here to illustrate the conclusions made based on these tests. A 6" sphere measured result is shown in Figure 4a at 18 GHz and vertical polarization. This should be compared with the 6" disk measured result shown in Figure 4b. These two results were measured directly using the previously described system. Using this raw data, one is not simply examining the effect of the target alone in that the styrofoam pedestal also generates a forward scatter as shown in Figure 5. In order to eliminate this effect, a styrofoam pattern was taken alone; then, the target was measured. The styrofoam result was then subtracted from the target return so that only the target forward scatter is present. The subtracted 6" sphere and 6"

disk results are shown in Figures 6a and b, respectively. One should note the similarity in the results as suggested by the aperture blockage model. Next a 2' long by 4" diameter cylinder and plate were measured with both targets mounted perpendicular to the link line-of-sight and horizontally oriented relative to the ground as shown in Figure 2b. The raw measured results are shown in Figures 7a and b and the subtracted ones in Figures 8a and b. Again note that these two targets have essentially the same forward scatter. A 1/20th scale model of a 737 aircraft was also measured as shown in Figure 1. The raw measured results at 18 GHz for vertical and horizontal polarizations are shown in Figures 9a and b, respectively; whereas, the subtracted ones are shown in Figures 10a and b. It is interesting here to compare the scattering pattern shapes for the two polarizations since the aperture blockage concept is not sensitive to polarization. Again, the results indicate that the aperture blockage concept is correct.

The 737 aircraft results were simulated using the numerical solution by Rudduck and Lee [1]. The model used to simulate the 737 is shown in Figure 11. It is a rather crude representation but models the basic features. Note that this scattering model is simply a flat plate with the cross-section shown in the previous figure. The calculated and measured raw results are shown in Figure 12, and the subtracted ones are shown in Figure 13. These two results do not perfectly agree but show the same characteristic behaviour. It is felt that these results could be improved with a better 737 representation. In any event, it is clear that the major effect associated with an aircraft breaking a ground

station-to-satellite link is the aperture blockage caused by the structure physically blocking the line-of-sight signal.

There was some interest in determining how much energy was flowing around the aircraft. In order to study this effect, the range was set up to obtain three frequency scans from 12 to 18 GHz. Separate scans were taken for the styrofoam pedestal, a 6" sphere, and the 737 aircraft. This data was then calibrated using the following expression:

$$\text{Calibration} = \left[ \frac{737 - \text{styrofoam}}{6'' \text{ sphere-styrofoam}} \right] \text{Exact } 6'' \text{ Sphere} .$$

Using this calibration formula at each frequency the forward scattering of the 737 aircraft can be isolated. The calibrated frequency data was then windowed and transformed to the time domain. The time domain result represents the forward scattering of the 737 for a very short pulse illumination. If energy propagates significantly around the target there should be a delayed signal associated with the transit time it takes to propagate around the object. This time response is shown in Figure 14, and one should note that there does not appear to be any significant multipath or terms propagating around the target. It is simply the direct line-of-sight blockage which is observed in the time response. As a result, this data also verifies the aperture blockage concept which implies that Rudduck and Lee's [1] numerical solution is valid for this type of problem.

## III. THEORETICAL SOLUTION

The theoretical solution used for the aircraft forward scattering recently developed for calculating the scattering effects of reflector antenna feeds is shown in Figure 15. When the scatterer is located inside the projected aperture, and close to the antenna a simple Geometrical Optics (GO) model is used as shown in Figure 15a. However, if the scatterer is lcoated outside the projected aperture as shown in Figure 15b, the GO model is not adequate. In the latter case, the actual antenna near fields incident upon the scatterer need to be calculated over the appropriate scattering aperture. Then the resulting near fields are integrated to obtain the forward scattering. The resulting integration is performed over an extended aperture. Thus, the basic analysis is called the Extended Aperture Integration (AIE) method, as shown in Figure 16. GTD is used at close to medium distances between the antenna and scatterer; whereas, AI is used for large distances.

An example which demonstrates the application to reflector feed scattering is shown in Figure 17. The computer model uses the equivalent plate scatterer for the feed and mast scattering as shown in Figure 18. The measured and calculated patterns, as shown in Figures 19 and 20, illustrate the validity of this approach.

The aircraft scattering was also modelled by equivalent plate scatterers as shown in Figure 21. The complete set of calculated data will be presented in a future report; however, a few sample calculations

are shown in the following tables. The equivalent plate that was used to represent a C5 aircraft is shown in Figure 22. Each table shows the unblocked reflector gain, the gain level of the aircraft scattering, the blocked reflector gain, and the resulting gain loss. Tables I and II show results for a 20-foot diameter reflector for 10 GHz and 20 GHz, respectively. Table III shows results for a 60-foot reflector at 4 GHz. As can be seen the aircraft scattering can cause a substantial gain loss.

A simplified theoretical solution was developed to calculate the aircraft scattering at large distances (approximately in the far field of the ground station antenna). This simplified solution provides more insight and greatly improves the efficiency over the computer code. The simplified solution can be used if the blockage model can be represented by rectangular plates as shown in Figure 23. The calculated gain data for a simplified (one plate) blockage model is given in Table IV which represents the minimum blockage of the C5; whereas, the two plate model or maximum blockage of the C5 is given in Table V. In all cases if a large aircraft directly flies through a ground station-satellite link, there can be a drop in the system gain. What effect this has on the system is dependent on the system under consideration. However if the aircraft is in the near field of the ground station, the gain loss is substantial, and one would assume that the link would be lost during the time period the aircraft blocks the line-of-sight signal.

## REFERENCE

[1] R.C. Rudduck and T.H. Lee, Reflector Antenna Code under development for NASA Langley Research Center.

TABLE I

GAIN DATA FOR C5 AIRCRAFT SCATTERING

Reflector Diameter = 20.0'

Frequency = 10.0 GHz

C5 Aircraft

---

Case 1) Range = 1600.0'

( Use Near Field Data )

| | $\theta$ = 0 degree DB | phase (degrees) |
|---|---|---|
| a) Reflector only | 53.17 | -6.2 |
| b) Aircraft Scattered | 52.87 | -3.6 |
| c) Total | 28.05 | -56.76 |

Gain Loss = 53.17-28.05 = 25.12 DB

---

Case 2) Range = 41000.0' ( based on 3 DB-BW range )

( Use Far Field Data )

| | $\theta$ = 0 degree DB | phase (degrees) |
|---|---|---|
| a) Reflector only | 53.17 | -6.2 |
| b) Aircraft Scattered | 51.48 | 31.7 |
| c) Total | 48.95 | -61.35 |

Gain Loss = 53.17-48.95 = 4.22 DB

---

TABLE II

GAIN DATA FOR C5 AIRCRAFT SCATTERING

Reflector Diameter = 20.0'

Frequency = 20.0 GHz

C5 Aircraft

---

Case 1) Range = 80214.0' ( based on 3 DB-BW range )

( Use Far Field Data )

| | $\theta$ = 0 degree | |
|---|---|---|
| | DB | phase (degrees) |
| a) Reflector only | 59.19 | 77.6 |
| b) Aircraft Scattered | 58.18 | 102.8 |
| c) Total | 51.77 | 14.76 |

Gain Loss = 59.19-51.77 = 7.42 DB

---

TABLE III

GAIN DATA FOR C5 AIRCRAFT SCATTERING

Reflector Diameter = 60.0'

Frequency = 4.0 GHz

C5 Aircraft

Case 1) Range = 50134.0' ( based on 3 DB-BW range )

( Use Far Field Data )

| | $\theta$ = 0 degree DB | phase (degrees) |
|---|---|---|
| a) Reflector only | 54.75 | 169.2 |
| b) Aircraft Scattered | 47.48 | -136.6 |
| c) Total | 53.08 | 144.01 |

Gain Loss = 54.75-53.08 = 1.67 DB

TABLE IV

GAIN DATA FOR SIMPLIFIED BLOCKAGE (MINIMUM BLOCKAGE)

Reflector Diameter = 20.0'

Frequency = 10.0 GHz

Simple geometry test ( C5 Aircraft )

---

Geometry : Rectangular plate ( 240.0' X 20.0' )

---

Case 1) Range = 41000.0'

| | θ = 0 degree | |
|---|---|---|
| | DB | phase (degrees) |
| a) Reflector only | 53.17 | -6.2 |
| b) Aircraft Scattered | 42.20 | 31.2 |
| c) Total | 51.17 | -18.67 |

Gain Loss = 53.17-51.17 = 2.00 DB

Gain Loss ( Analytically Estimated ) = 1.95 DB

Phase Difference = -18.67-(-6.2) = -12.47 degrees

Phase Difference ( Analytically Estimated ) = -11.91 degrees

---

Case 2) Range = 410000.0'

| | θ = 0 degree | |
|---|---|---|
| | DB | phase (degrees) |
| a) Reflector only | 53.17 | -6.2 |
| b) Aircraft Scattered | 29.63 | 42.70 |
| c) Total | 52.79 | -9.19 |

Gain Loss = 53.17-52.79 = 0.38 DB

Gain Loss ( Analytically Estimated ) = 0.311 DB

Phase Difference = -9.19-(-6.2) = -2.99 degrees

Phase Difference ( Analytically Estimated ) = -6.23 degrees

---

TABLE IV (CONTINUED)

Case 3) Range = 4100.0'

| | $\theta$ = 0 degree | |
|---|---|---|
| | DB | phase (degrees) |
| a) Reflector only | 53.17 | -6.2 |
| b) Aircraft Scattered | 52.29 | 31.8 |
| c) Total | 49.10 | -68.84 |

Gain Loss = 53.17-49.10 = 4.07 DB

Gain Loss ( Analytically Estimated ) = 6.103 DB

Phase Difference = -68.84-(-6.2) = -62.64 degrees

Phase Difference ( Analytically Estimated ) = -66.09 degrees

## TABLE V

## GAIN DATA FOR SIMPLIFIED BLOCKAGE (MAXIMUM BLOCKAGE)

Reflector Diameter = 20.0'

Frequency = 10.0 GHz

Simple geometry test ( C5 Aircraft )

---

Geometry : 2 Rectangular plate

( 240.0' X 20.0' )
( 222.0' X 20.0' )

---

Case 1) Range = 41000.0'

| | θ = 0 degree DB | phase (degrees) |
|---|---|---|
| a) Reflector only | 53.17 | -6.2 |
| b) Aircraft Scattered | 48.20 | 22.9 |
| c) Total | 48.38 | -34.59 |

Gain Loss = 53.17-48.38 = 4.79 DB

Gain Loss ( Analytically Estimated ) = 4.80 DB

Phase Difference = -34.59-(-6.2) = -28.39 degrees

Phase Difference ( Analytically Estimated ) = -28.66 degrees

---

Case 2) Range = 410000.0'

| | θ = 0 degree DB | phase (degrees) |
|---|---|---|
| a) Reflector only | 53.17 | -6.2 |
| b) Aircraft Scattered | 34.96 | 43.6 |
| c) Total | 52.50 | -12.01 |

Gain Loss = 53.17-52.50 = 0.67 DB

Gain Loss ( Analytically Estimated ) = 0.48 DB

Phase Difference = -12.01-(-6.2) = -5.81 degrees

Phase Difference ( Analytically Estimated ) = -11.90 degrees

---

TABLE V (CONTINUED)

Case 3) Range = 4100.0'

| | $\theta$ = 0 degree | |
|---|---|---|
| | DB | phase (degrees) |
| a) Reflector only | 53.17 | -6.2 |
| b) Aircraft Scattered | 54.01 | 13.7 |
| c) Total | 44.67 | -101.70 |

Gain Loss = 53.17-44.67 = 8.50 DB

Gain Loss ( Analytically Estimated ) = 11.67 DB

Phase Difference = -101.70-(-6.2) = -95.50 degrees

Phase Difference ( Analytically Estimated ) = -137.55 degrees

ORIGINAL PAGE IS
OF POOR QUALITY

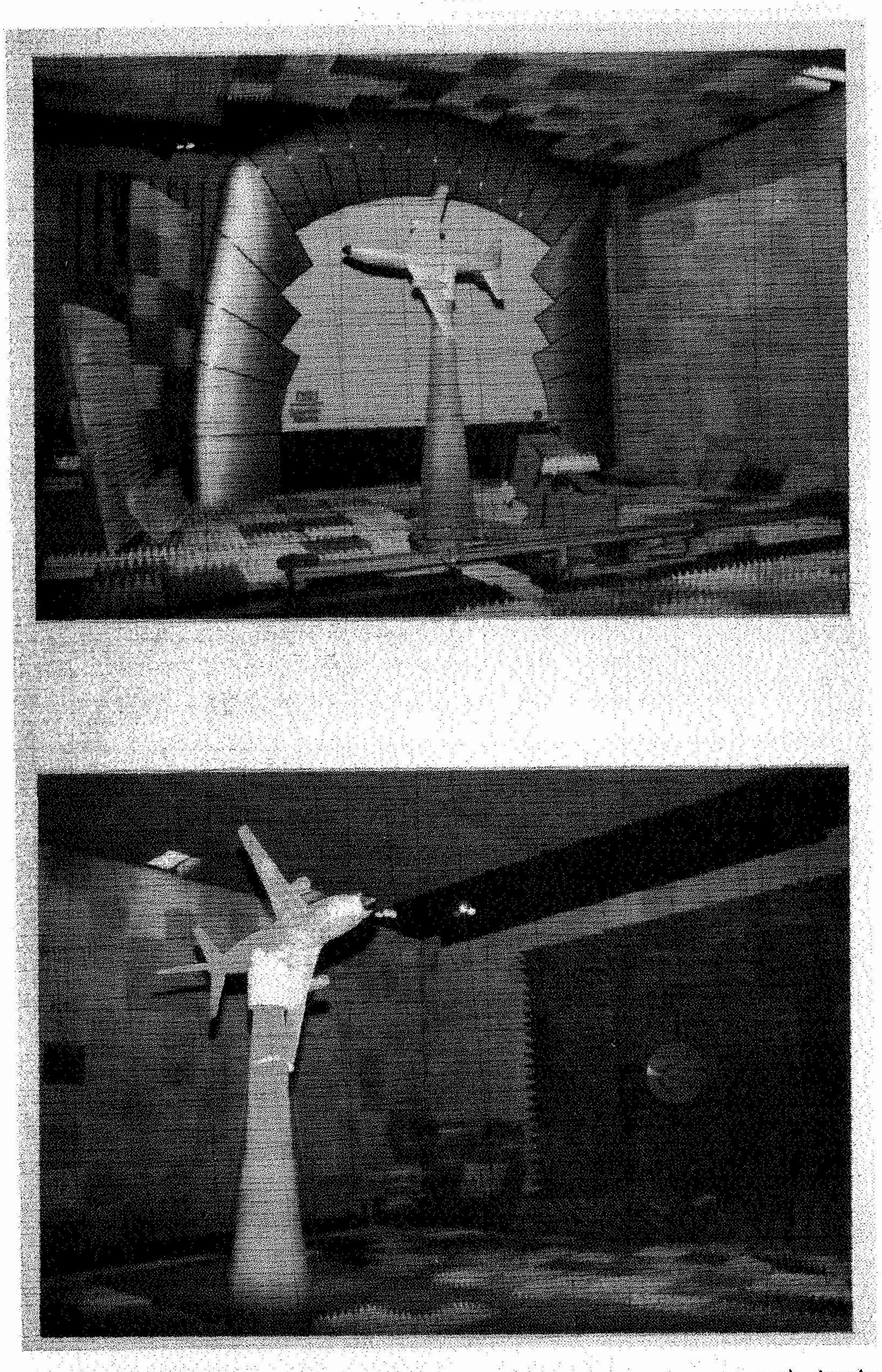

Figure 1. Measurement setup for the line-of-sight fly through tests.

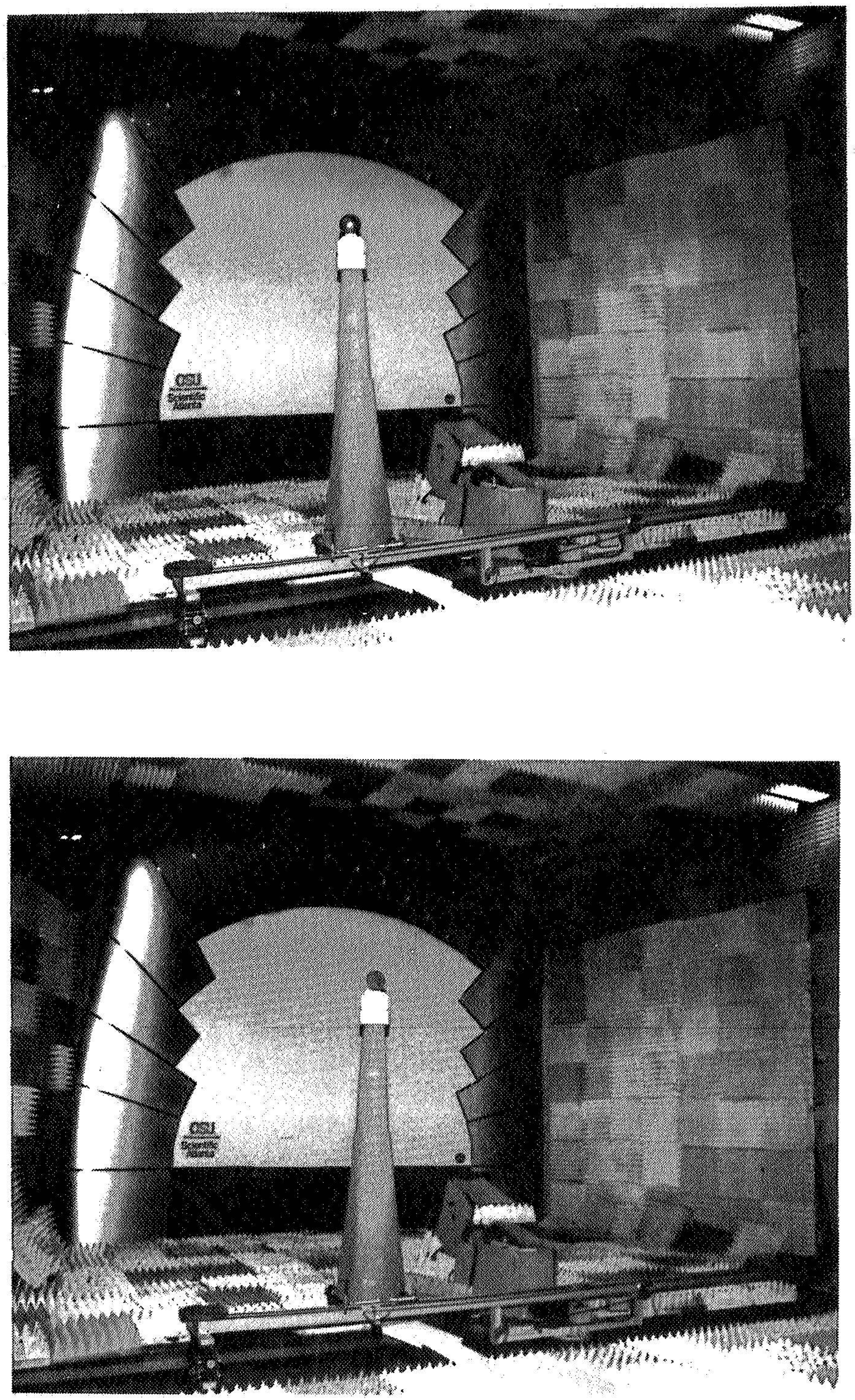

Figure 2a. Sphere and disk moving through the line-of-sight link.

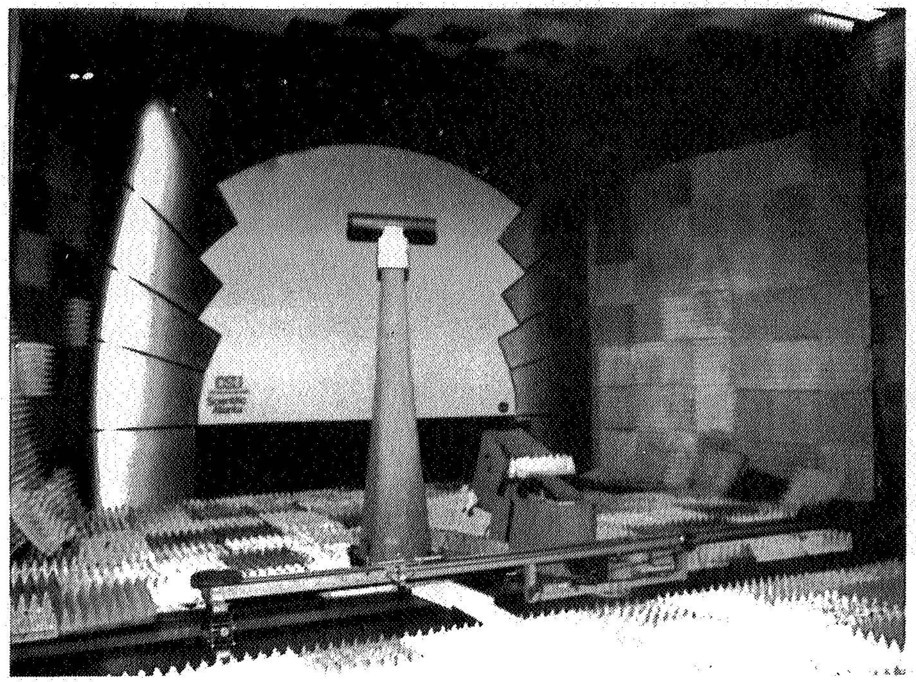

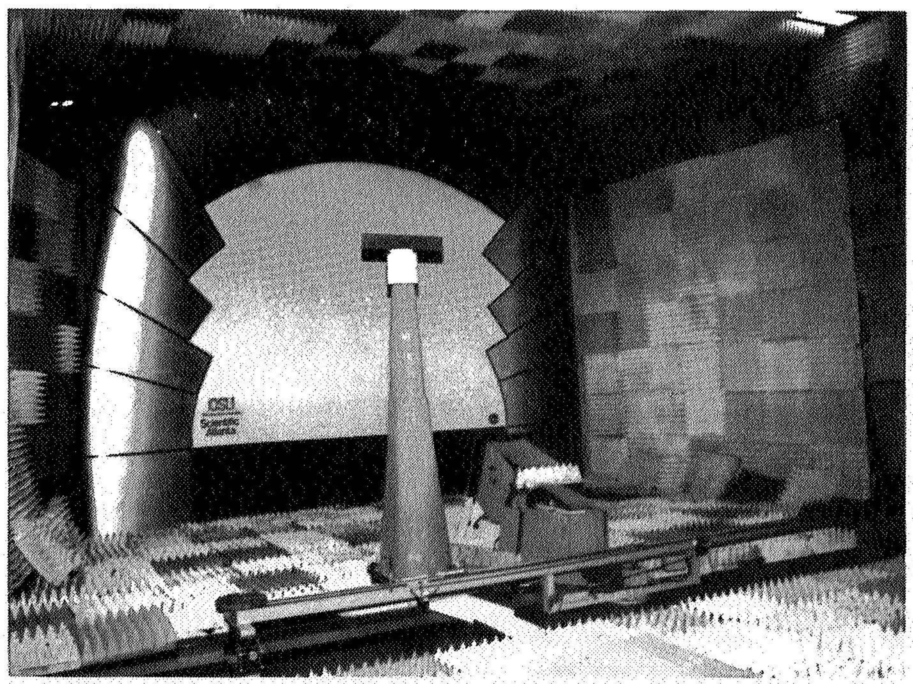

Figure 2b. Cylinder and plate moving through the line-of-sight link.

ORIGINAL PAGE IS
OF POOR QUALITY

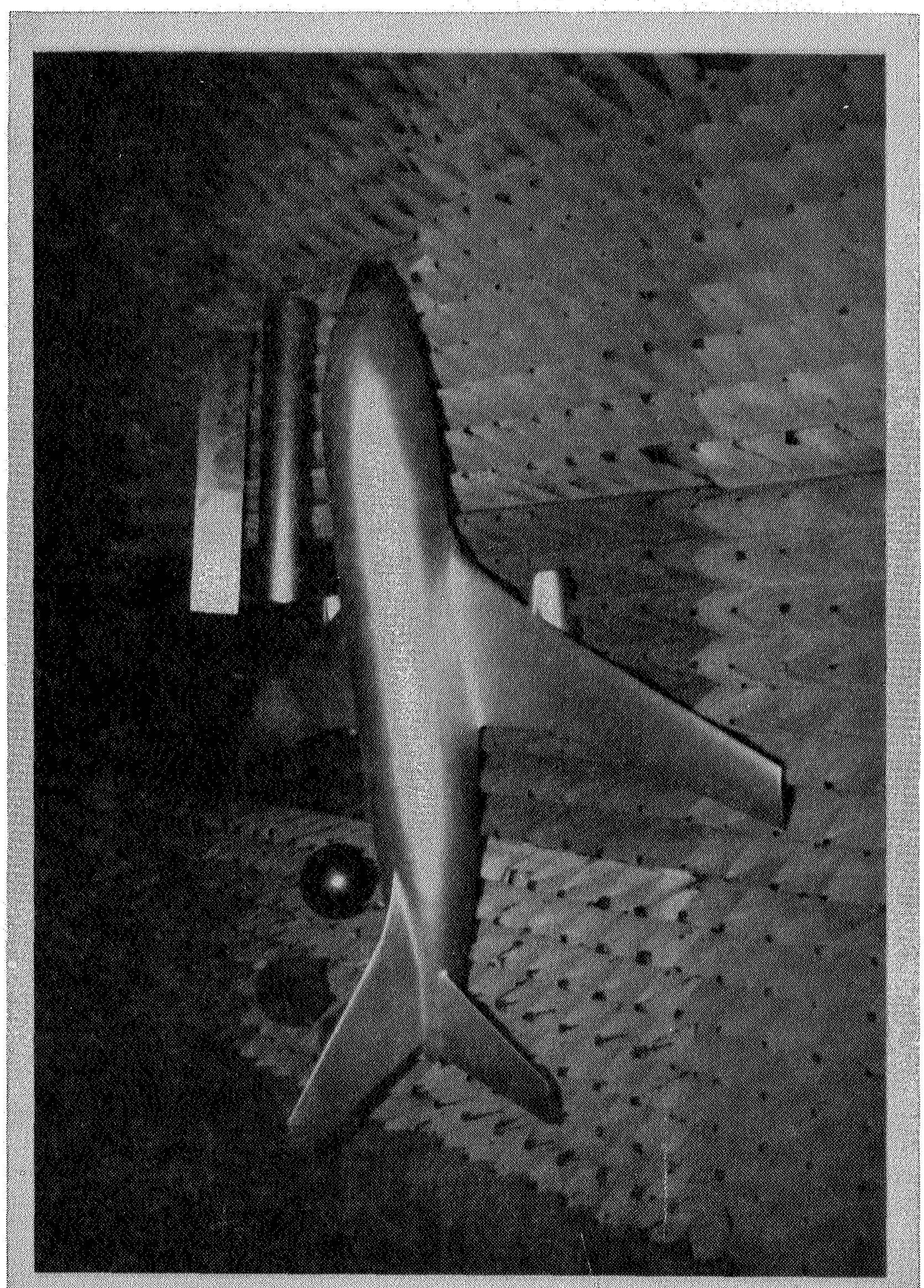

Figure 3. Some of the measured targets.

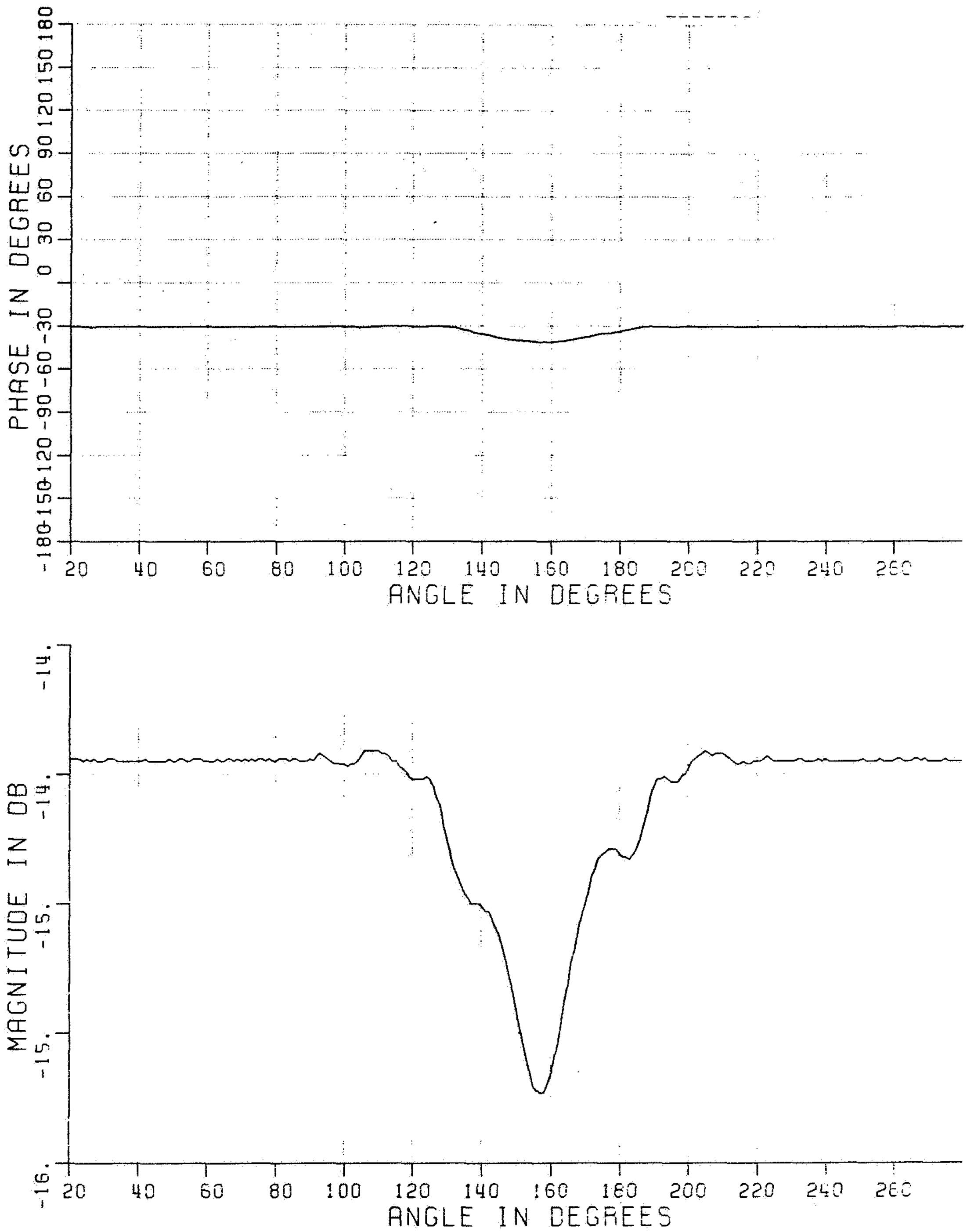


Figure 4a. Raw measured data for 6" sphere at 18 GHz and vertical polarization.

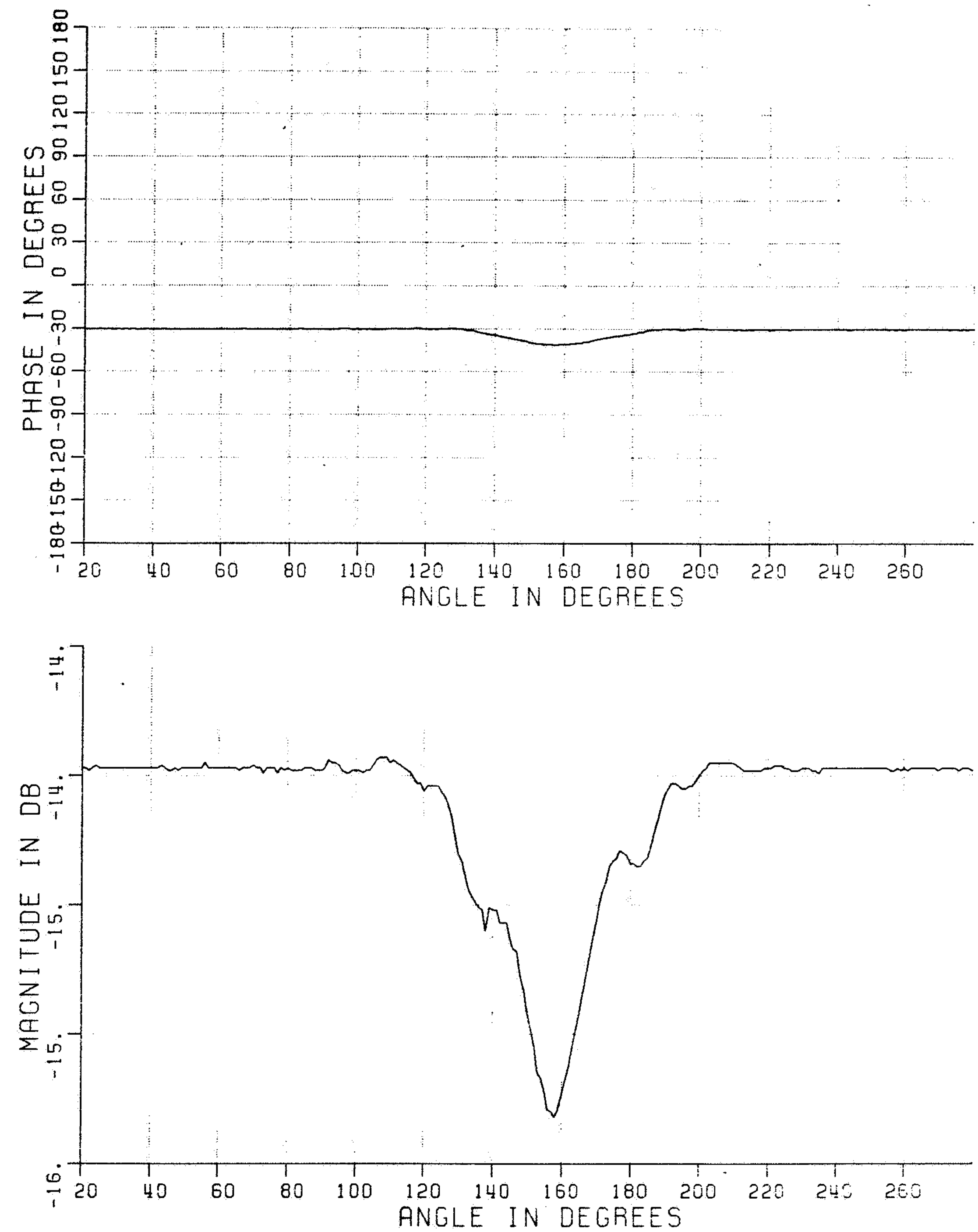


Figure 4b. Raw measured data for 6" disk at 18 GHz and vertical polarization.

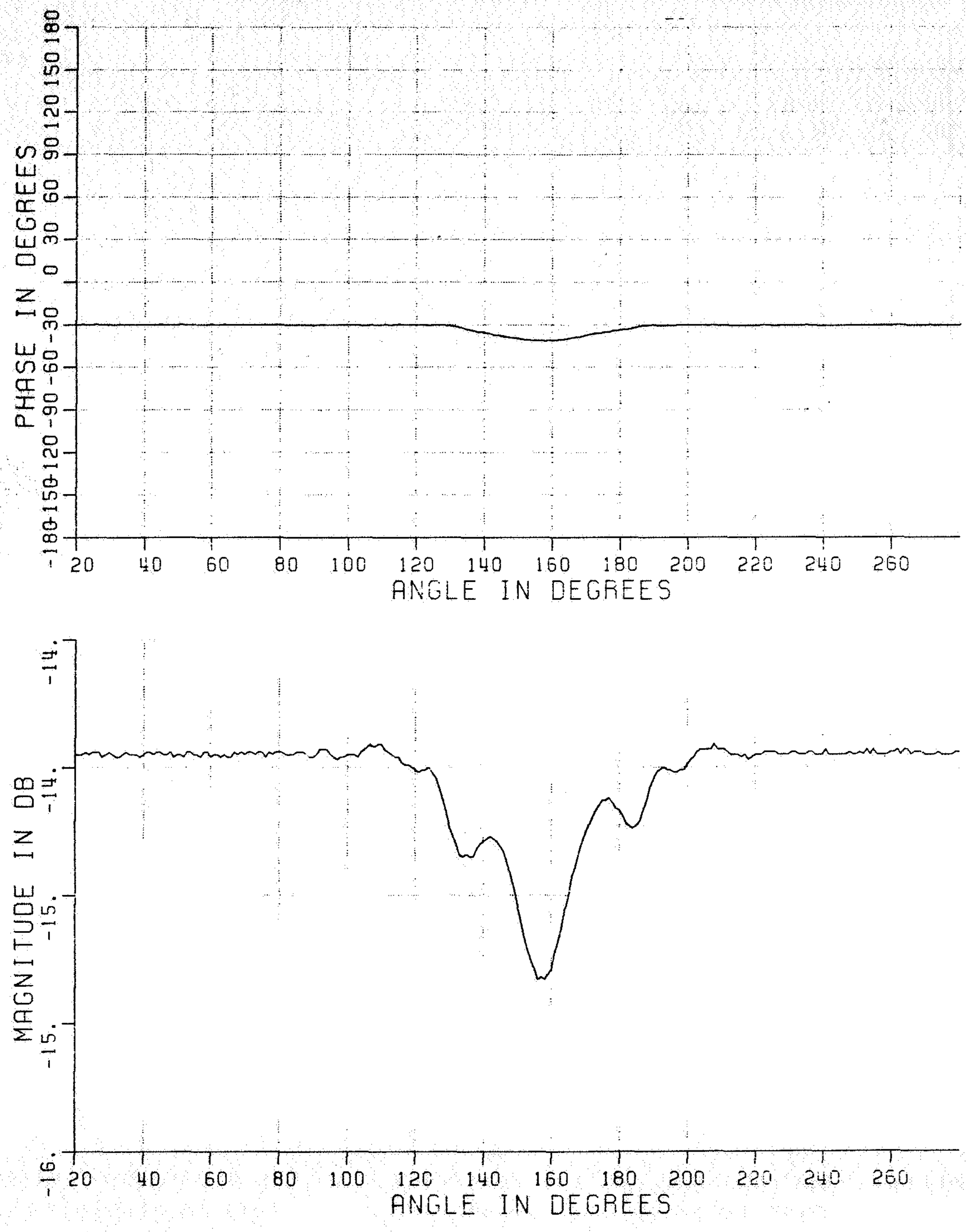


**Figure 5. Raw measured data for styrofoam pedestal at 18 GHz and vertical polarization.**

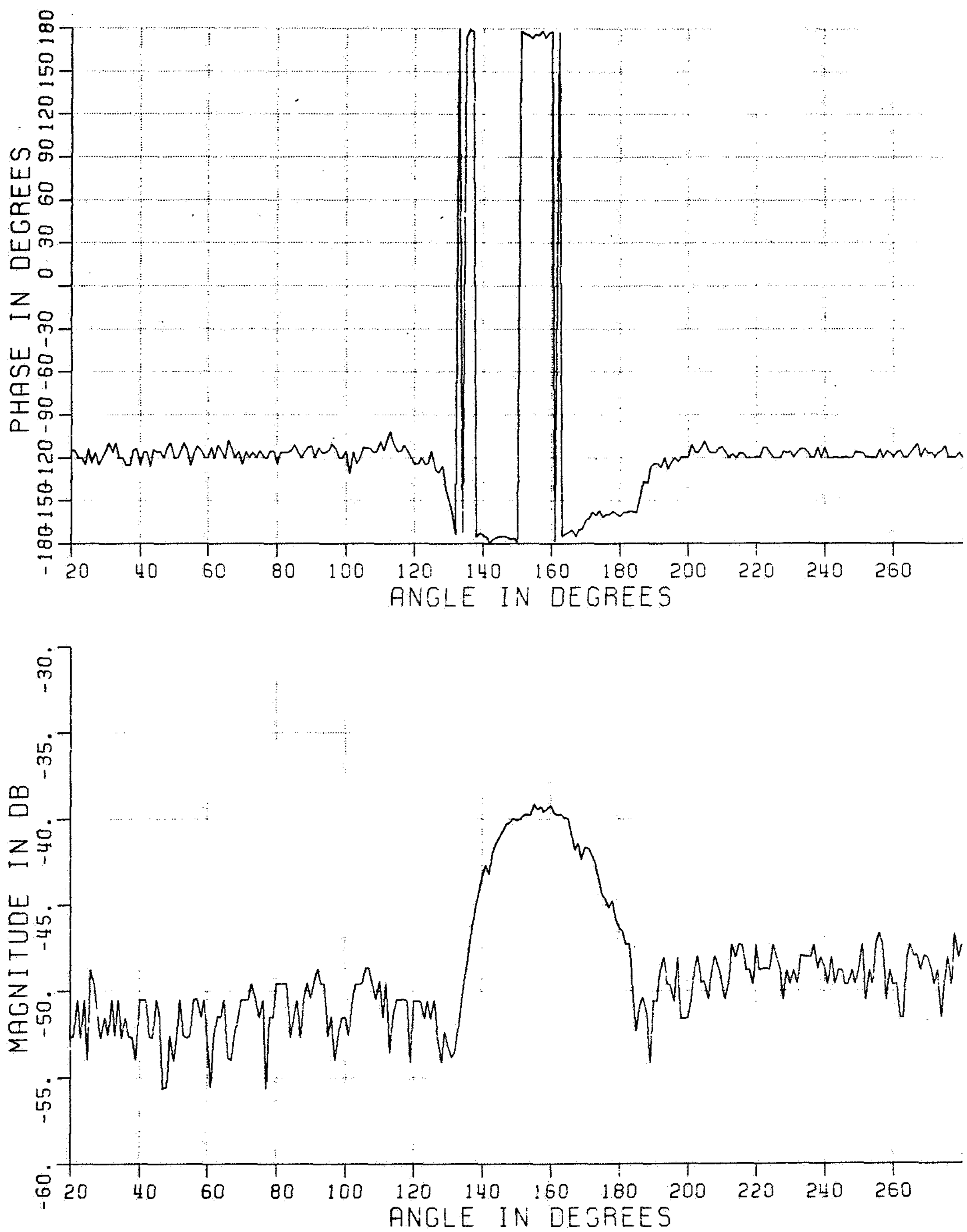


Figure 6a. Subtracted measured data for 6" sphere at 18 GHz and vertical polarization.

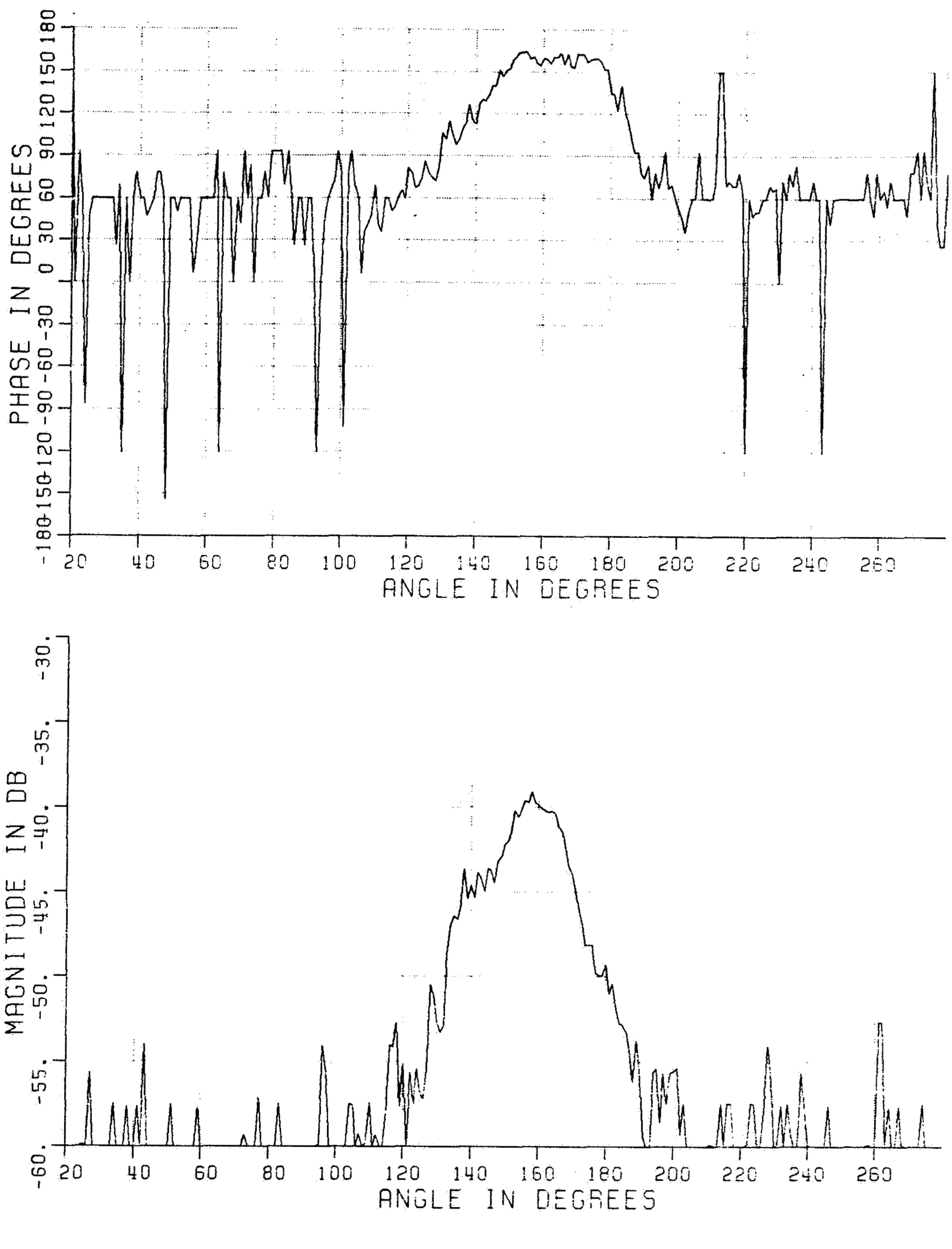


Figure 6b. Subtracted measured data for 6" disk at 18 GHz and vertical polarization.

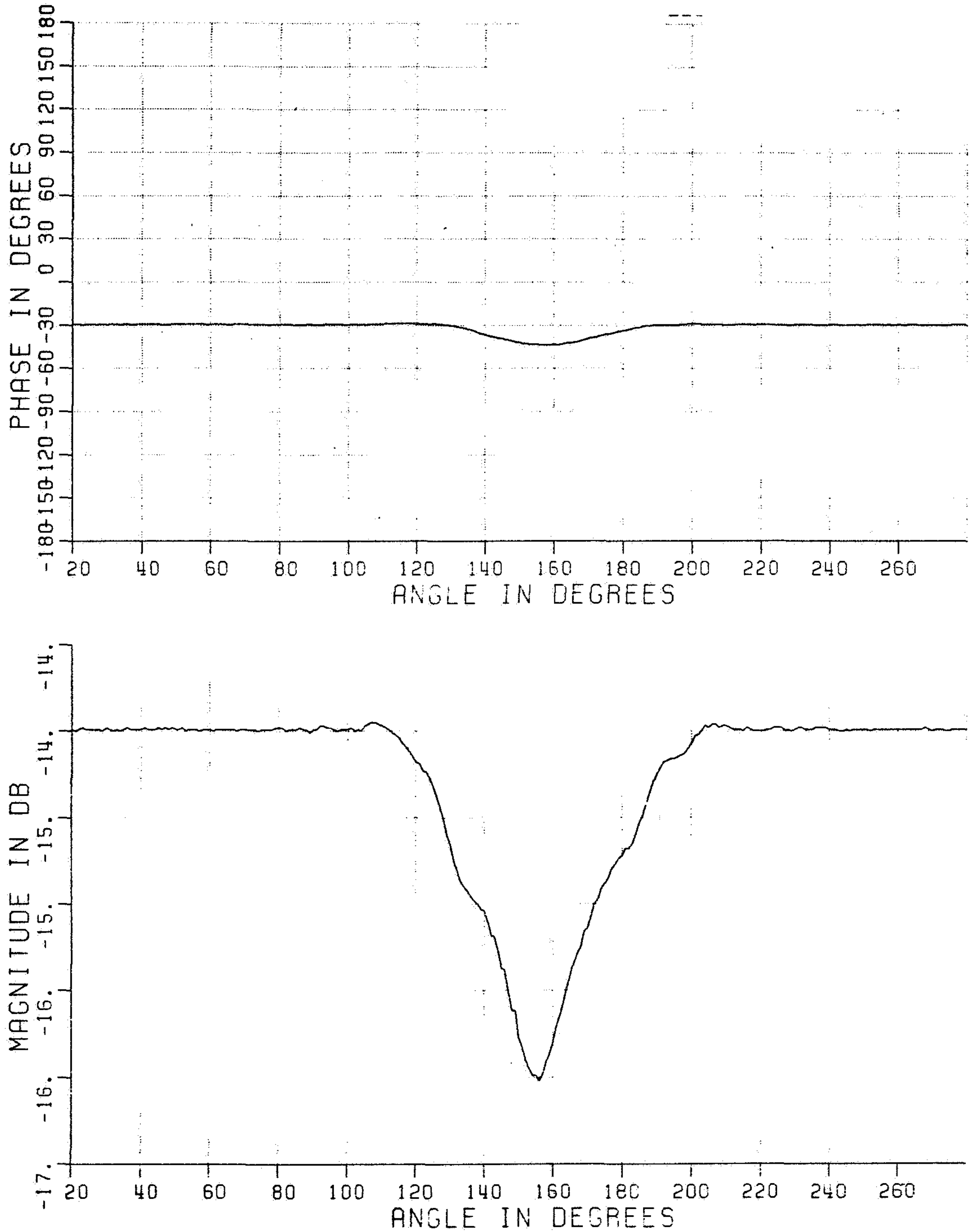


Figure 7a. Raw measured data for 2' x 4" cylinder at 18 GHz and vertical polarization.

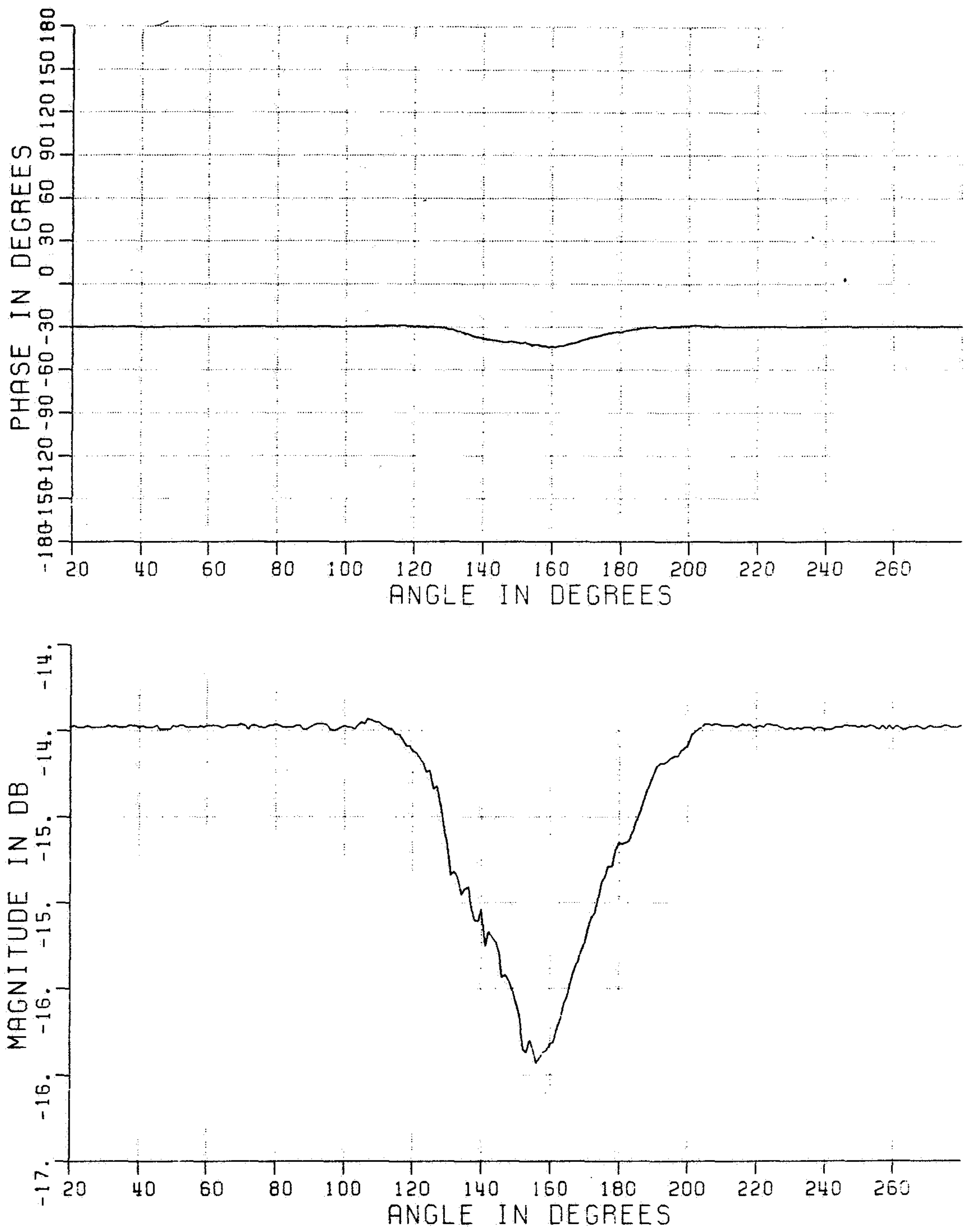


Figure 7b. Raw measured data for 2' x 4" plate at 18 GHz and vertical polarization.

ORIGINAL PAGE IS
OF POOR QUALITY

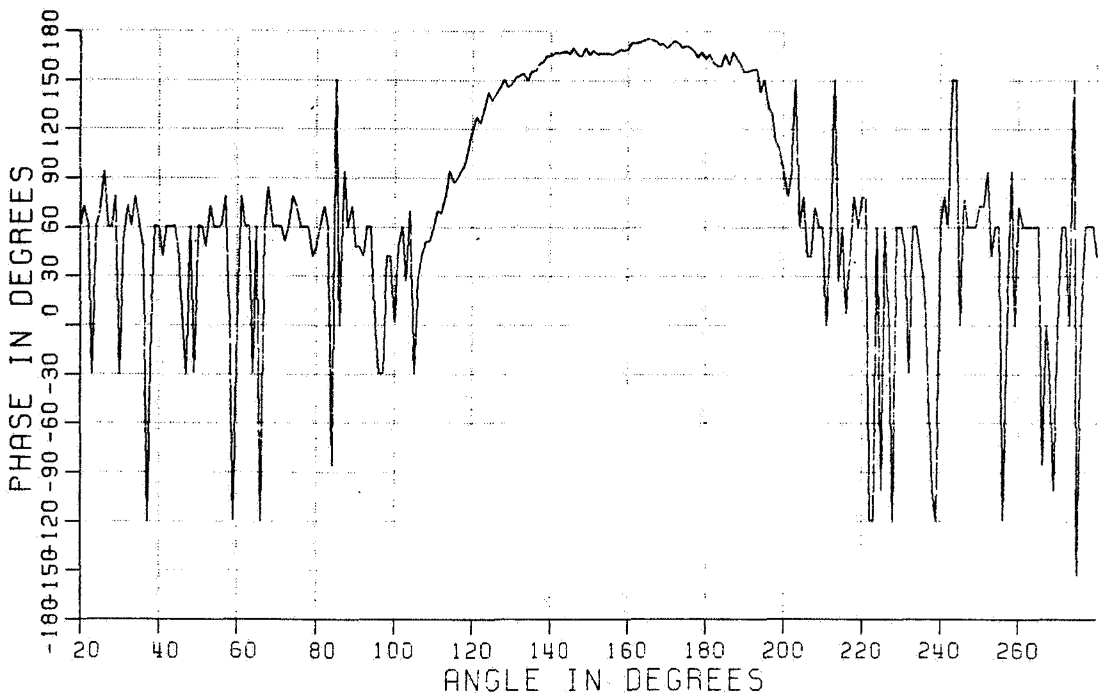


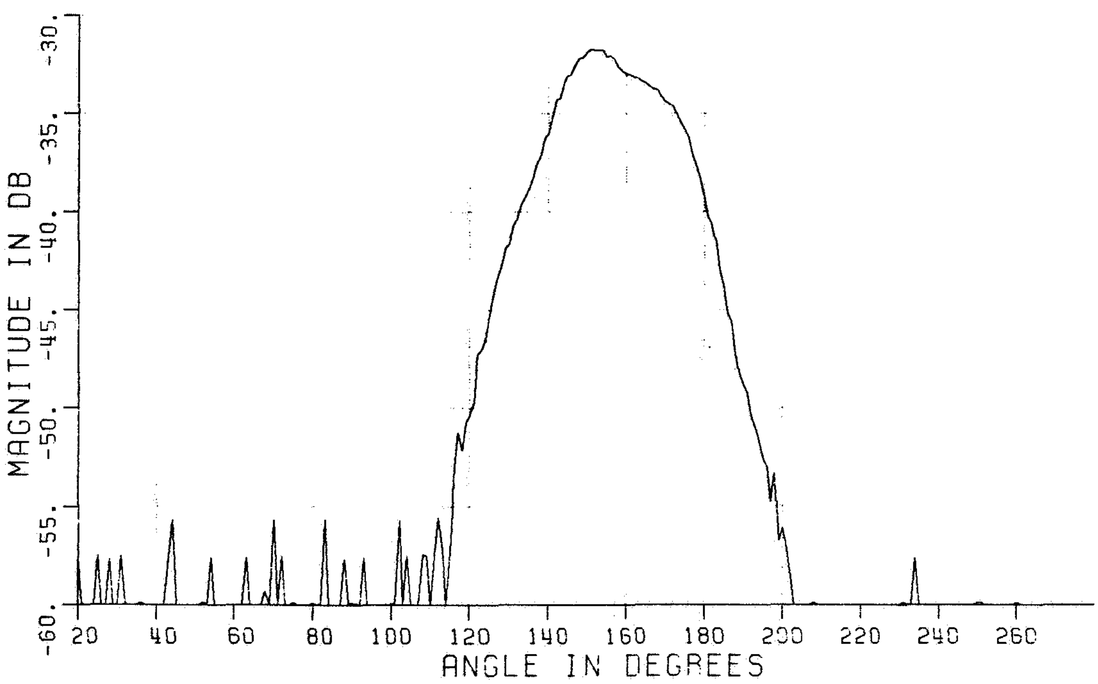


Figure 8a. Subtracted measured data for 2' x 4" cylinder at 18 GHz and vertical polarization.

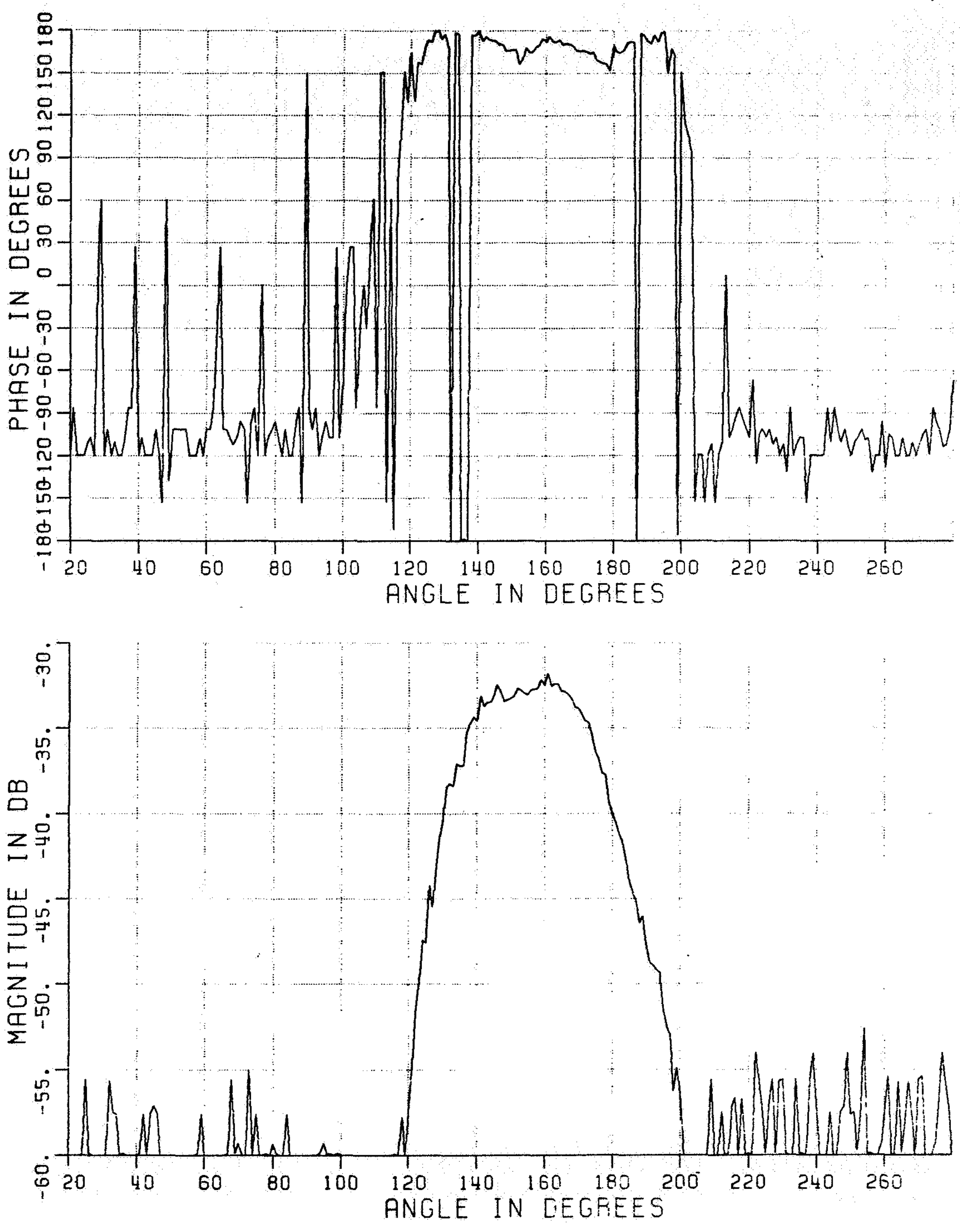


Figure 8b. Subtracted measured data for 2' x 4" plate at 18 GHz and vertical polarization.

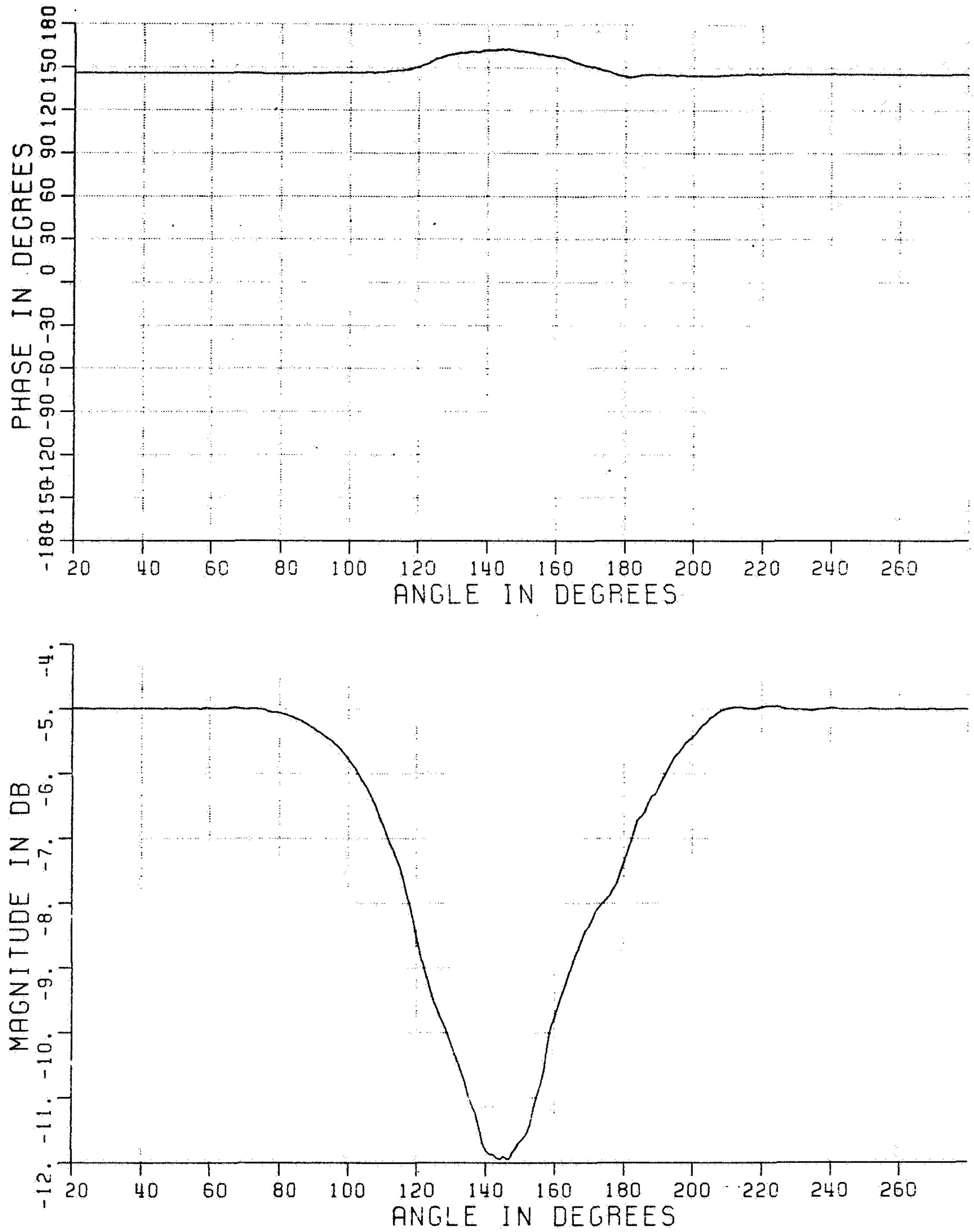


**Figure 9a.** Raw measured data for the 737 aircraft at 18 GHz and vertical polarization.

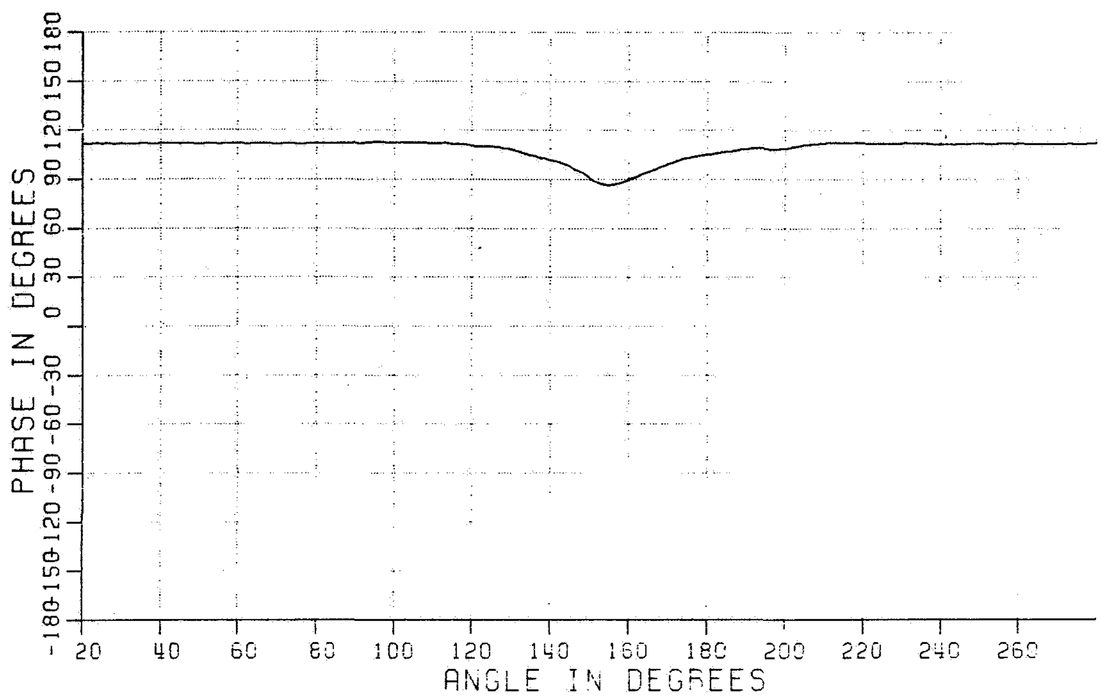


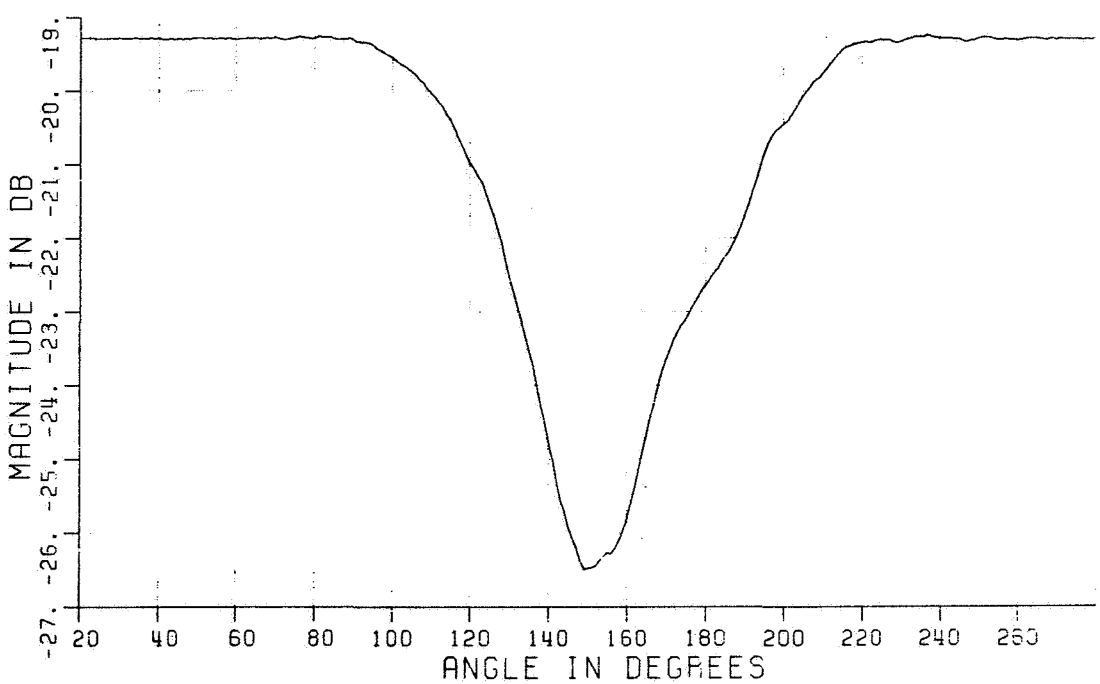


**Figure 9b. Raw measured data for 737 aircraft at 18 GHz and horizontal polarization.**

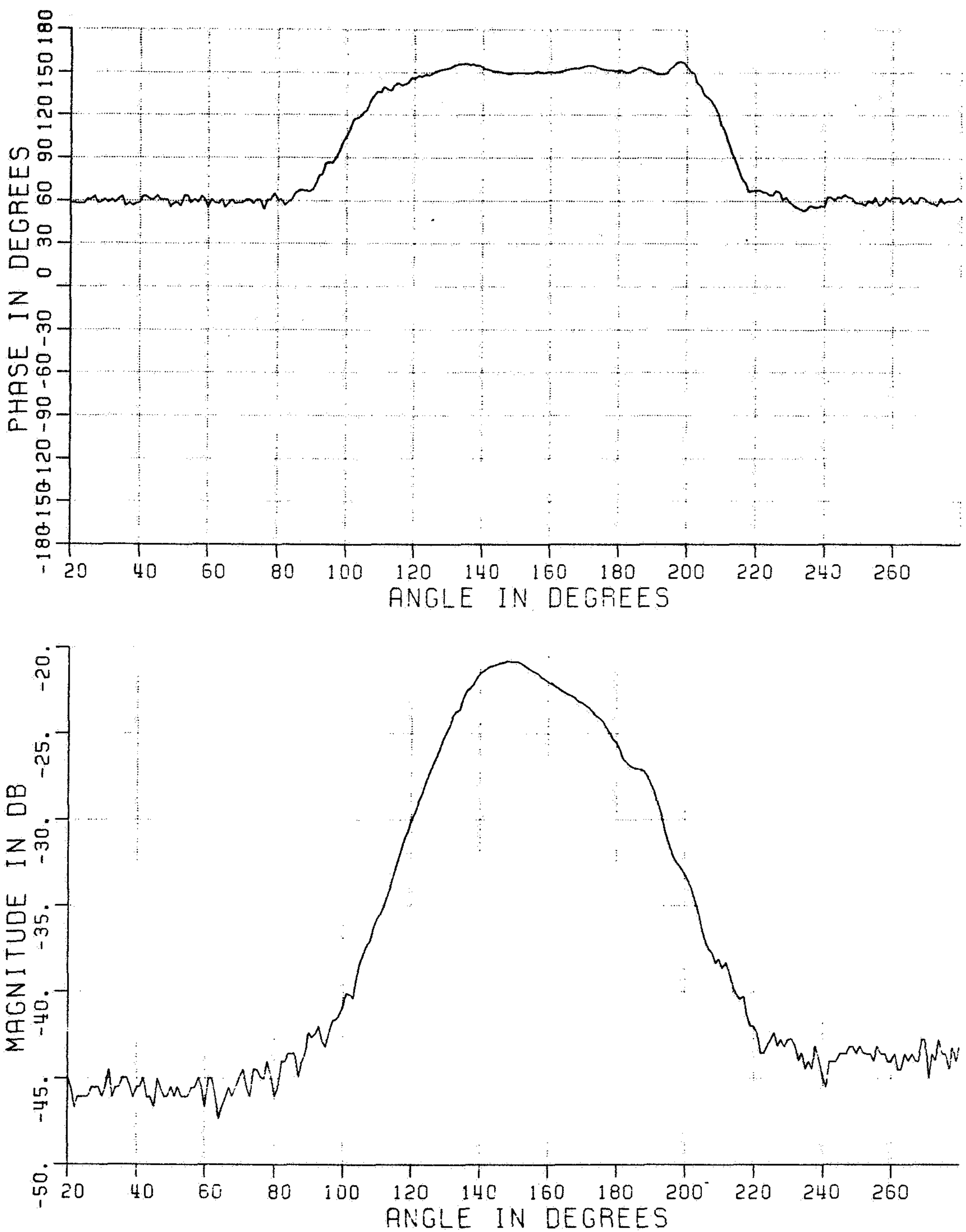


Figure 10a. Subtracted measured data for 737 aircraft at 18 GHz and vertical polarization.

ORIGINAL PAGE IS
OF POOR QUALITY

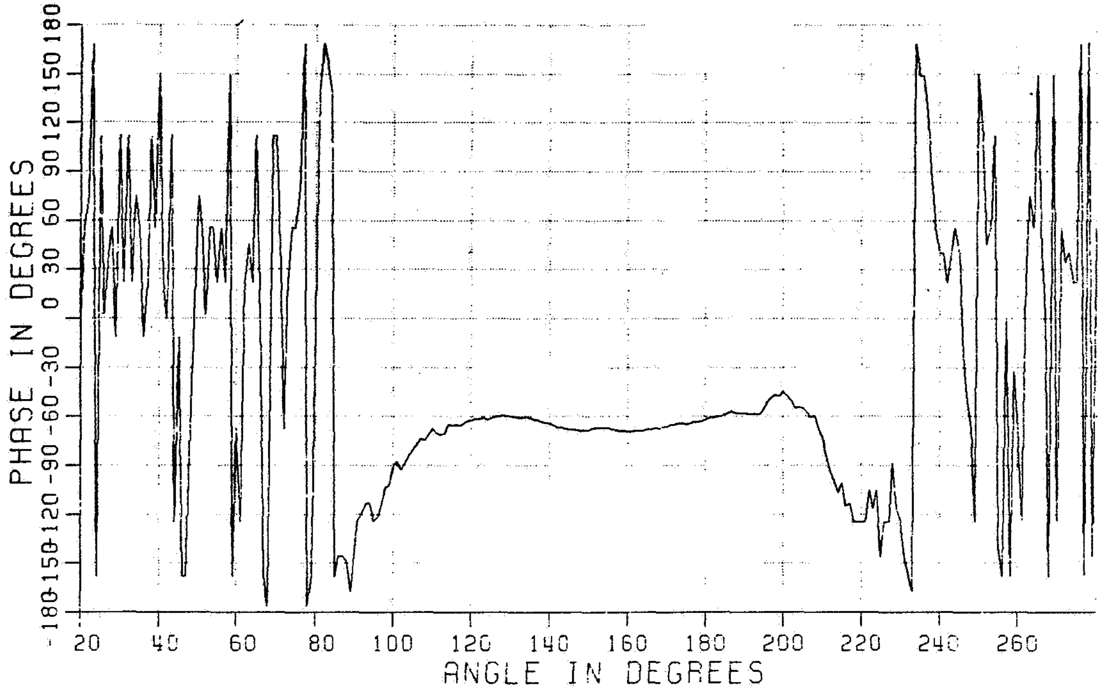


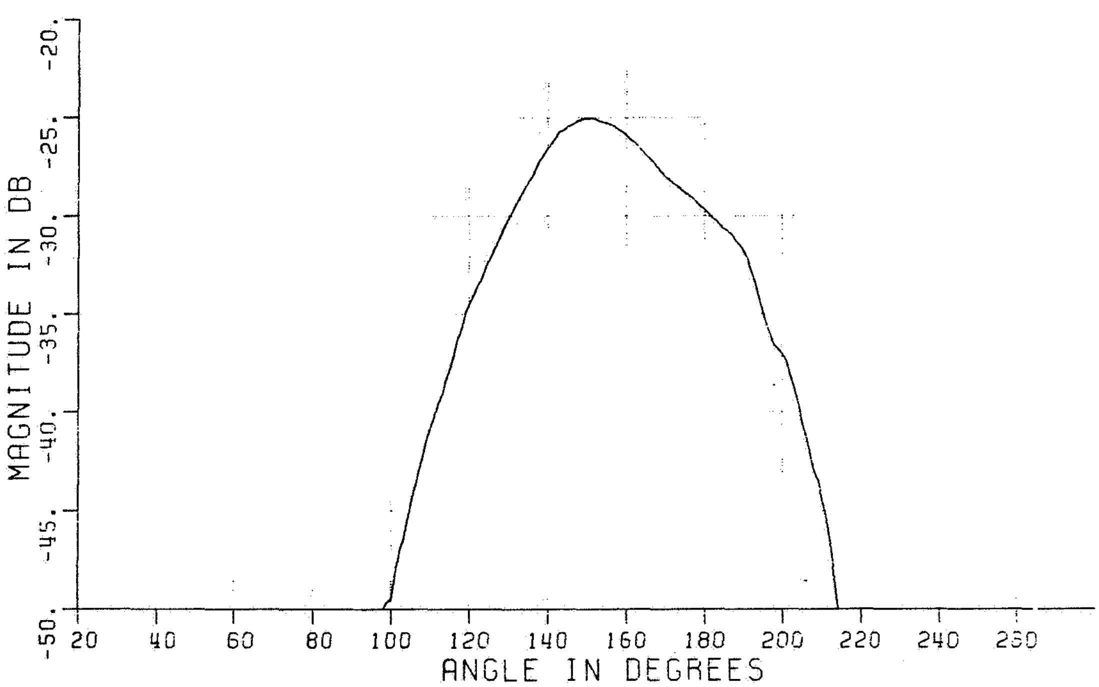


Figure 10b. Subtracted measured data for 737 aircraft at 18 GHz and horizontal polarization.

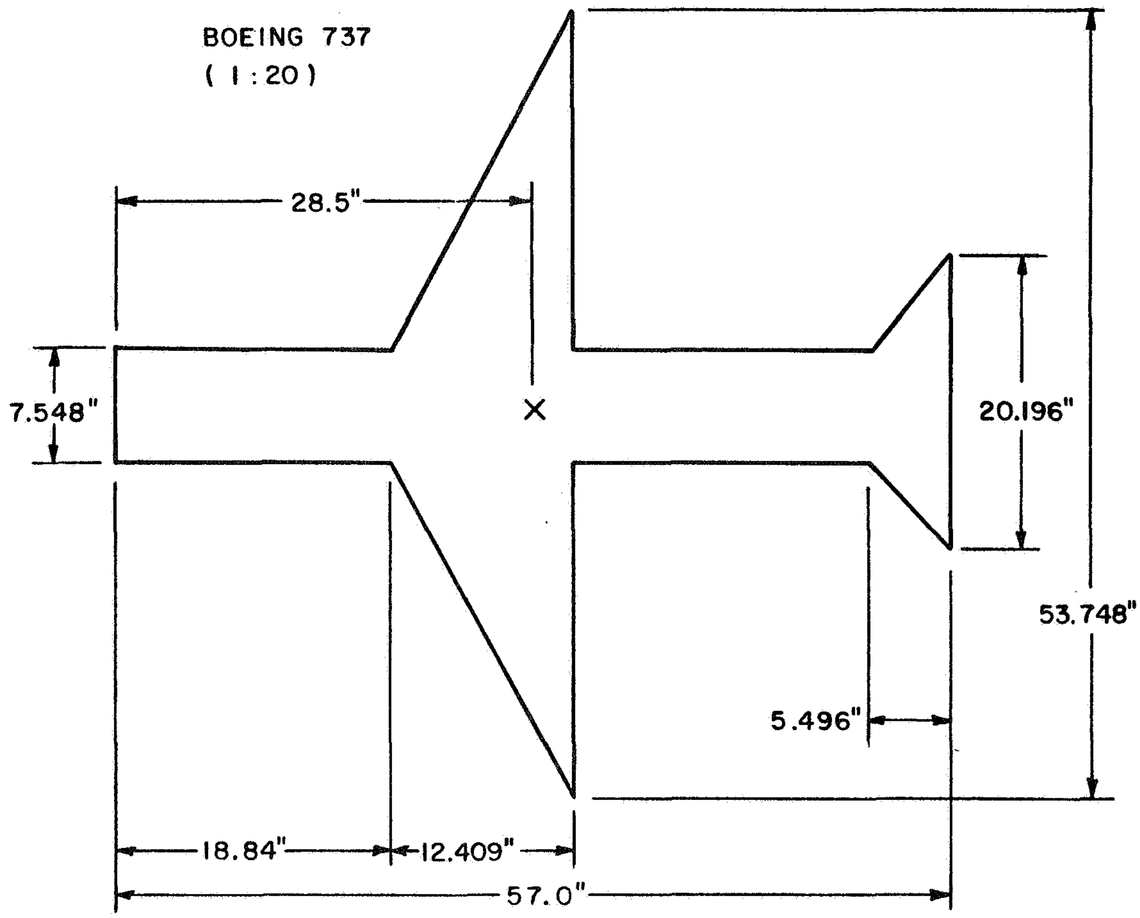


Figure 11. Simulated 737 aircraft used for calculations.

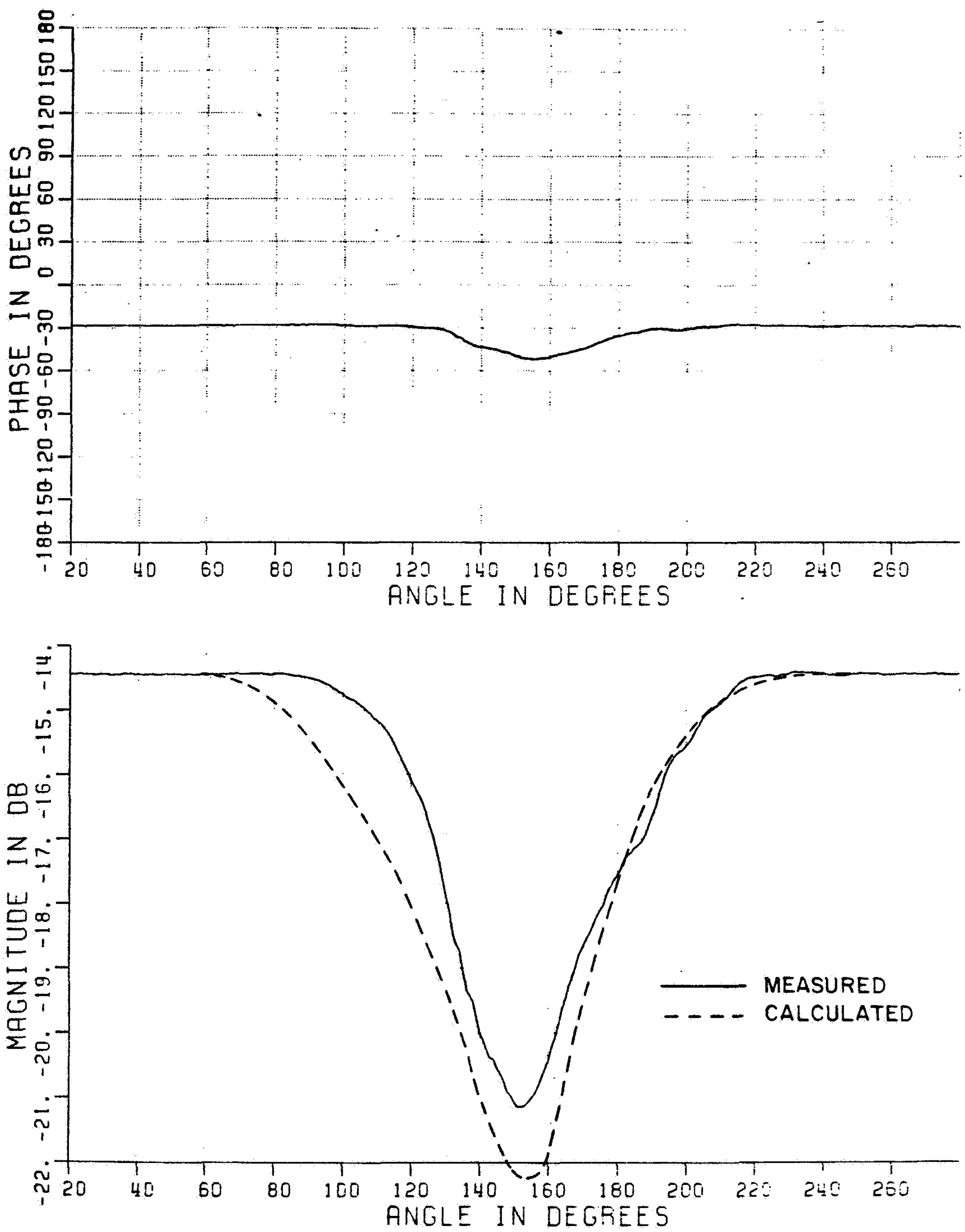


Figure 12. Calculated and measured raw data for 737 aircraft at 18 GHz and vertical polarization.

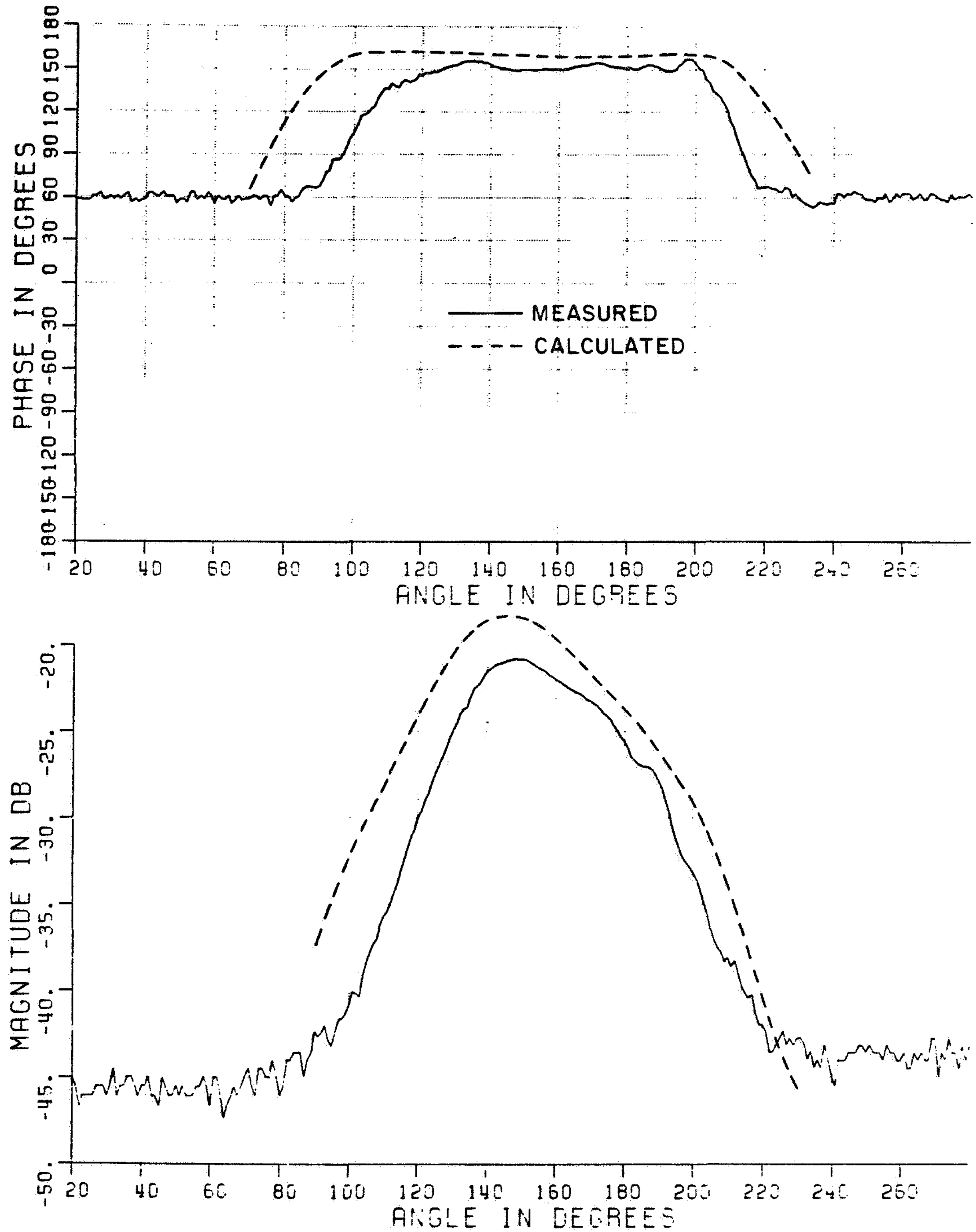


Figure 13. Calculated and measured subtracted data for 737 aircraft at 18 GHz and vertical polarizaiton.

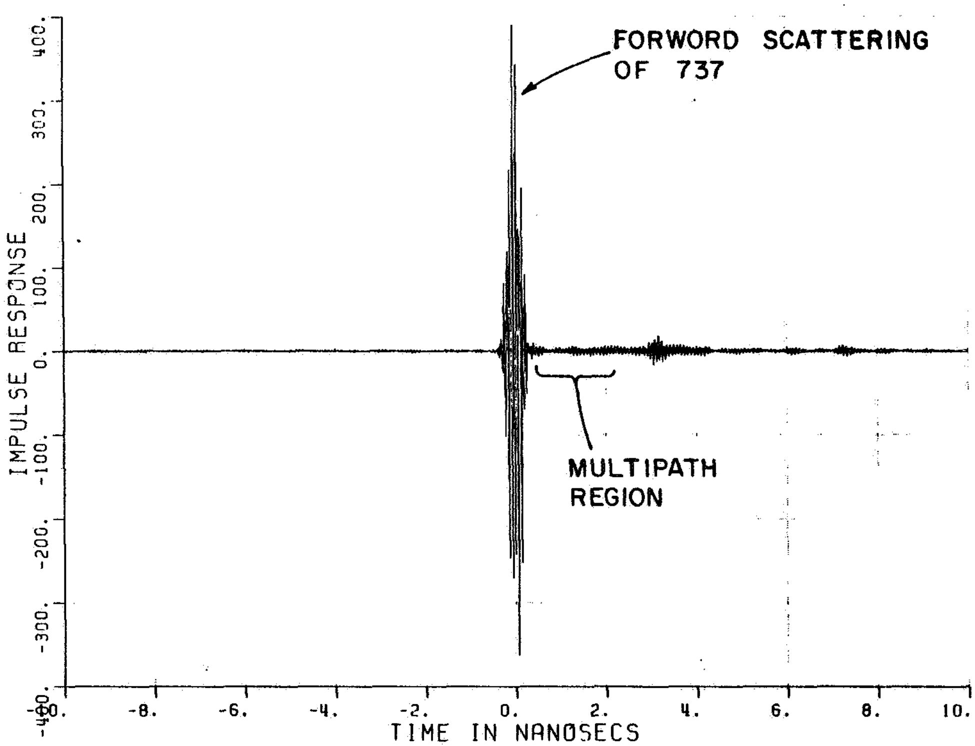


Figure 14. Time domain response for 737 aircraft.

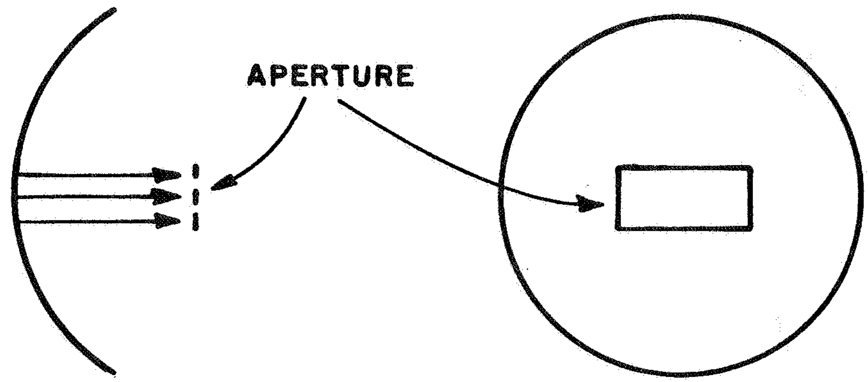


G.O. FIELDS IN APERTURE

(a) SCATTERER LOCATED INSIDE THE PROJECTED APERTURE

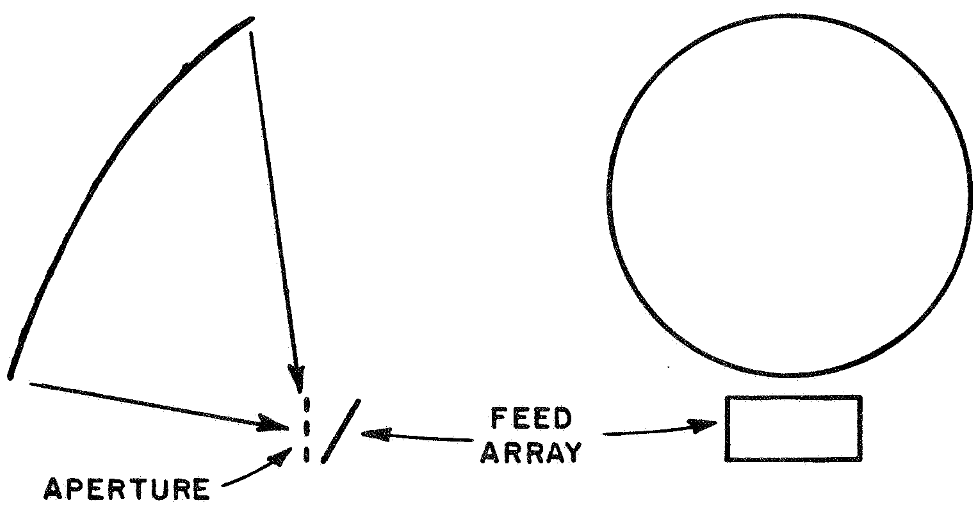


GTD DIFFRACTED FIELDS IN APERTURE

(b) SCATTERER LOCATED OUTSIDE THE PROJECTED APERTURE

Figure 15. Model for feed scattering calculation.

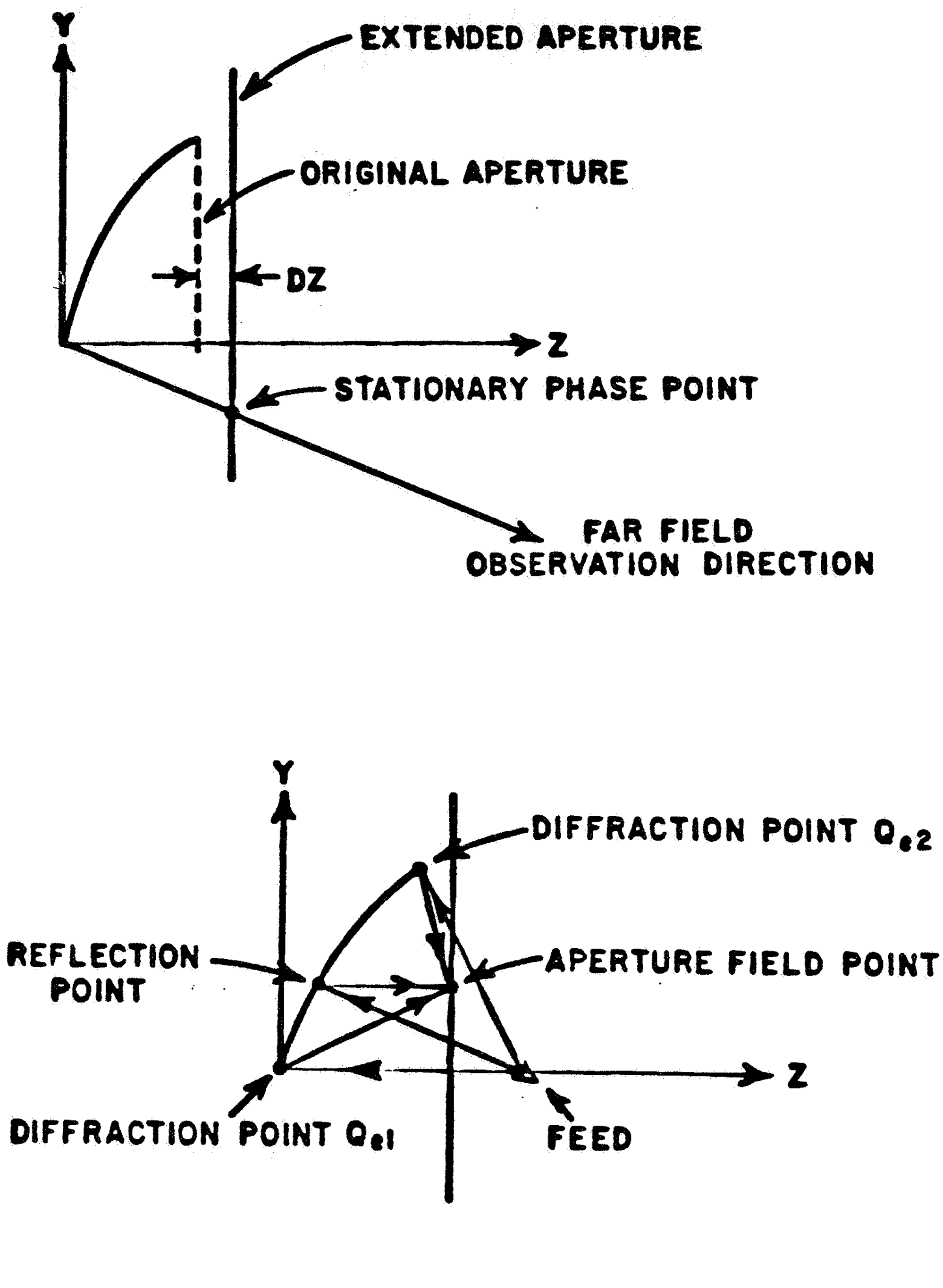


Figure 16. Extended Aperture Integration (AIE).

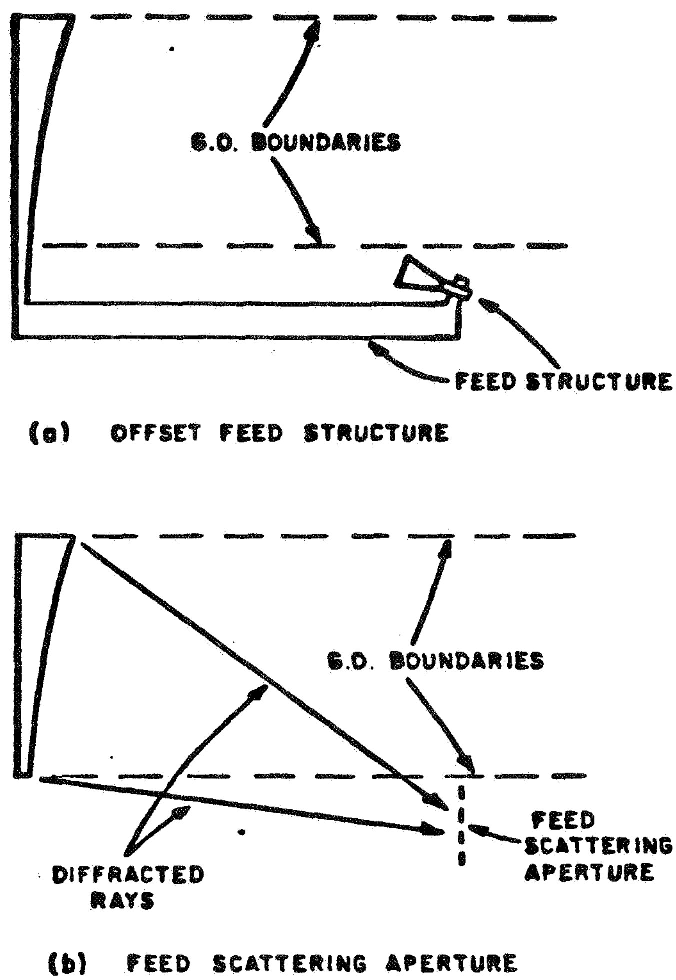


Figure 17. AIE method for feed scattering calcualtion.

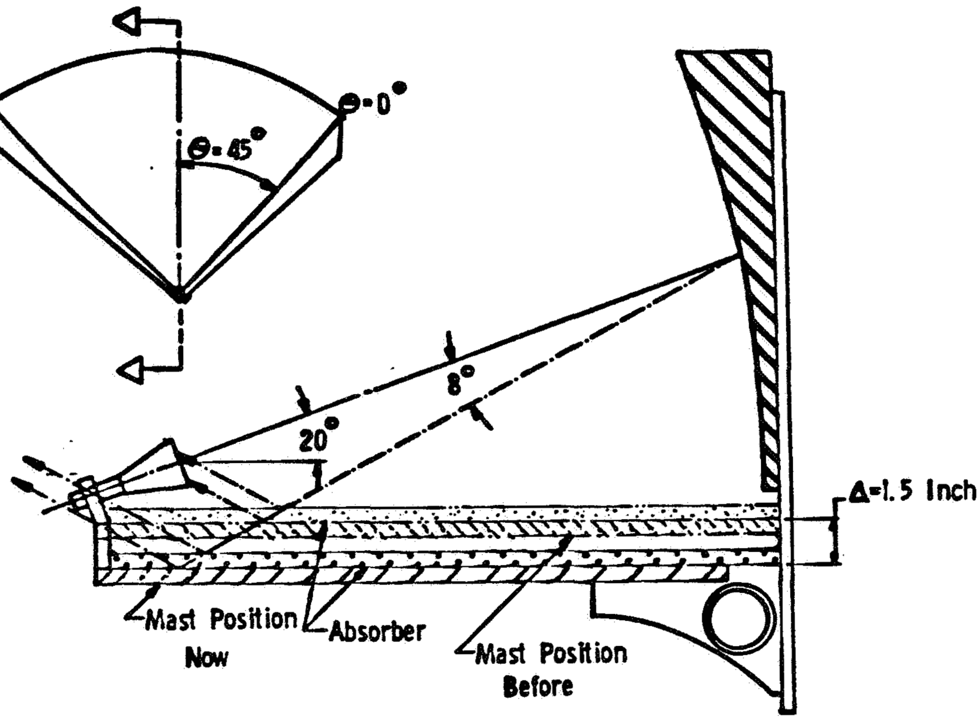


(a) Antenna with feed mast

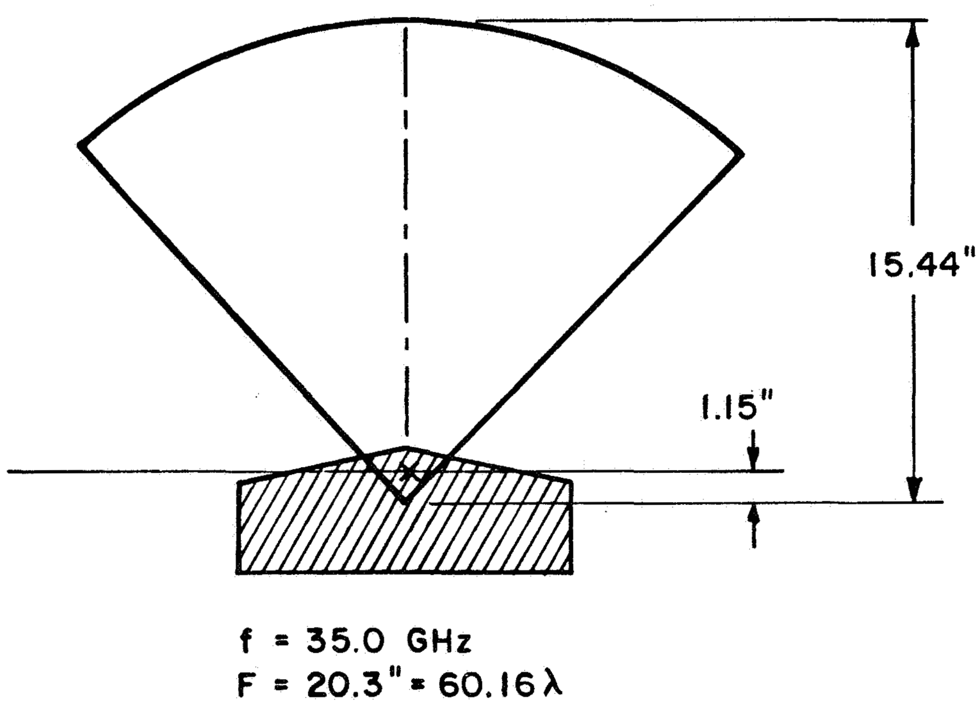


(b) Equivalent plate scatterer

Figure 18. Equivalent plate scatterer for the feed and mast.

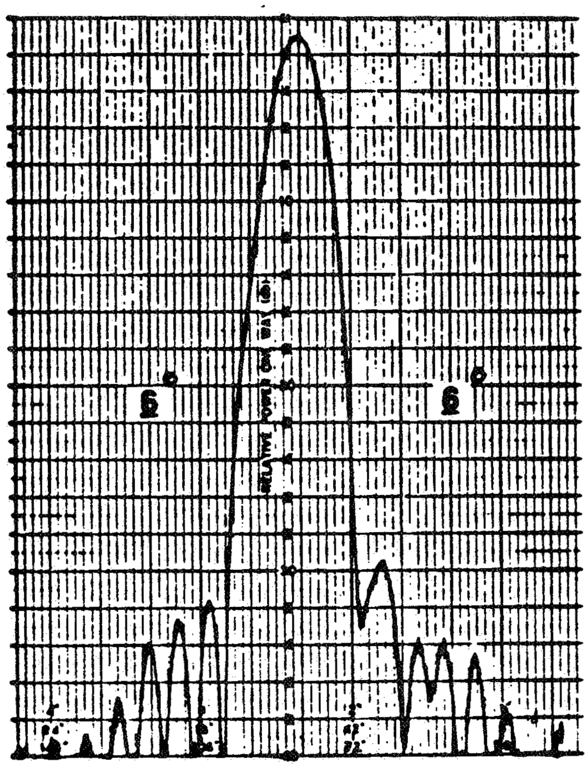

Figure 19. Measured E-plane pattern for the refelctor fo Figure 18.

f = 35 GHz.

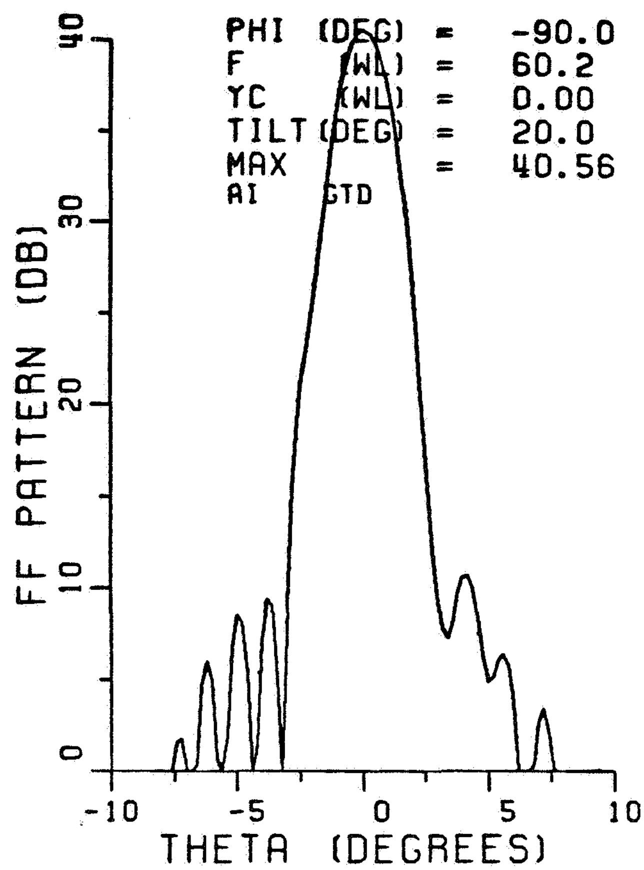


Figure 20. Calculated E-plane pattern for the reflector shown in Figure 18.

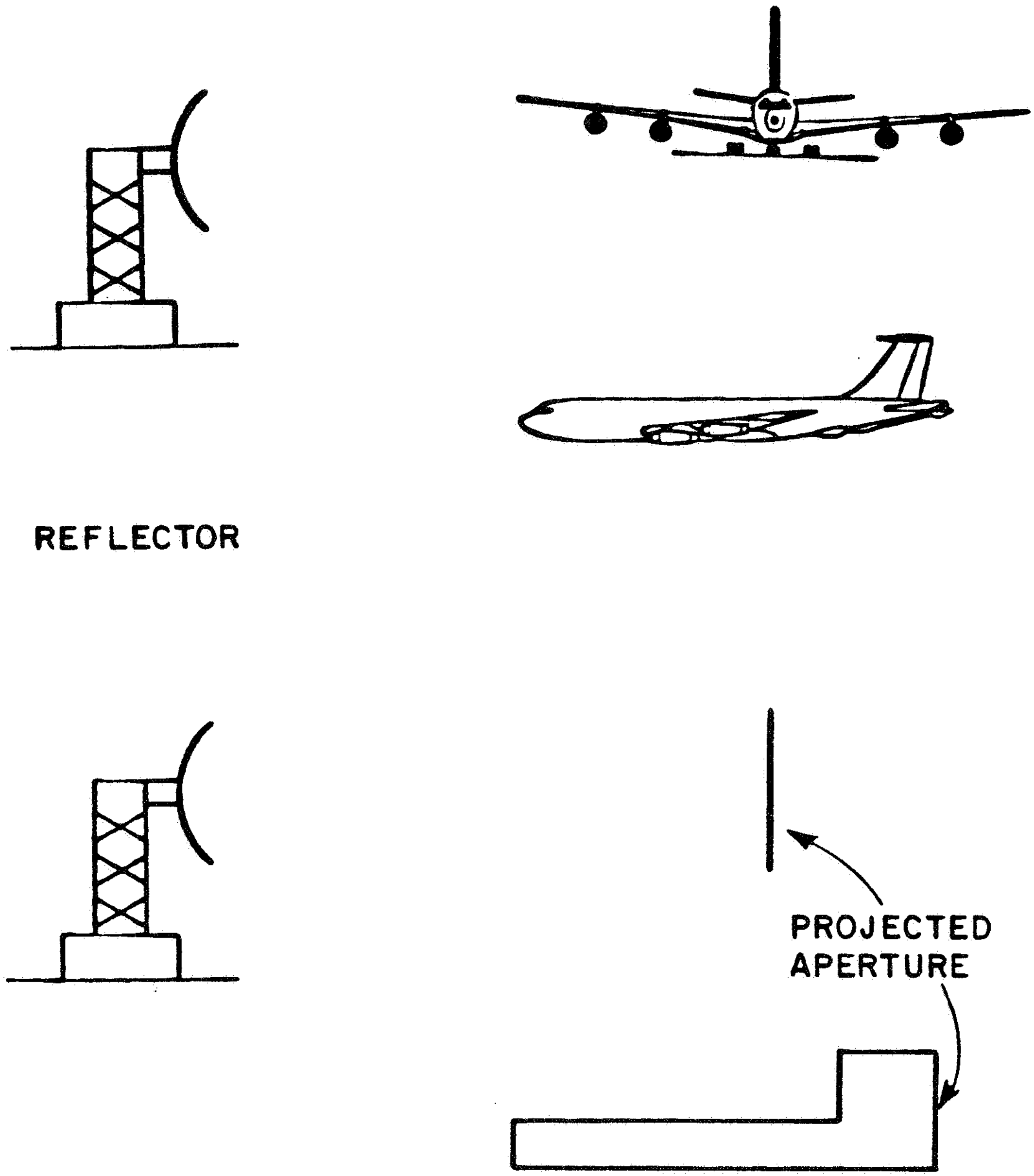


Figure 21. Equivalent plate for aircraft scattering model.

ORIGINAL PAGE IS
OF POOR QUALITY

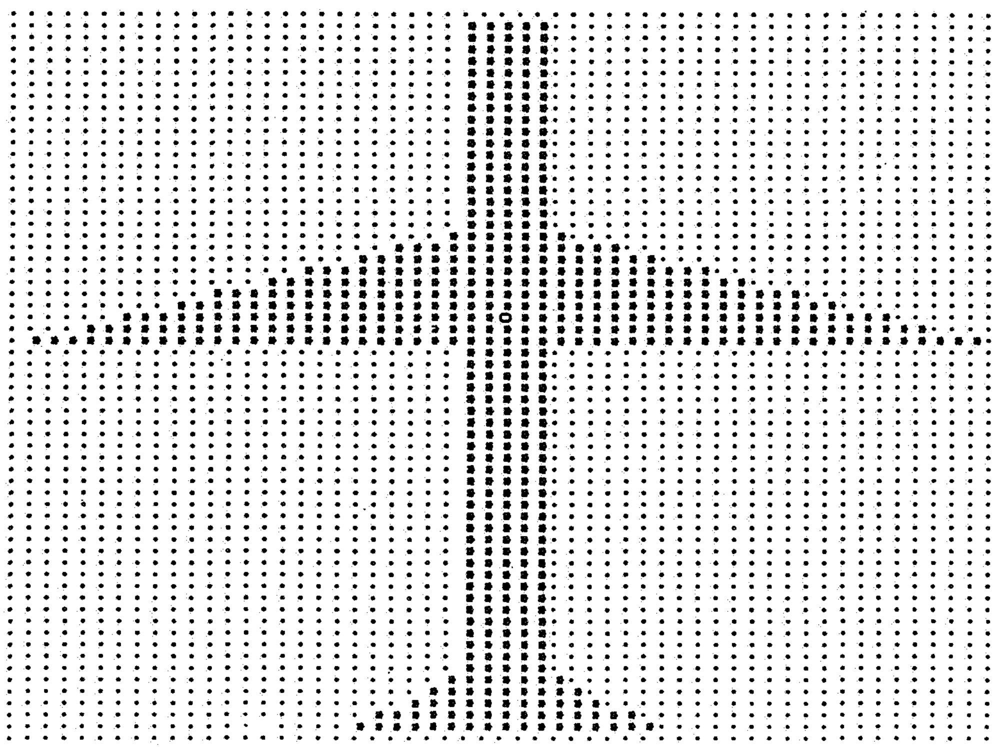

Figure 22. Equivalent plate for C5 aircraft.

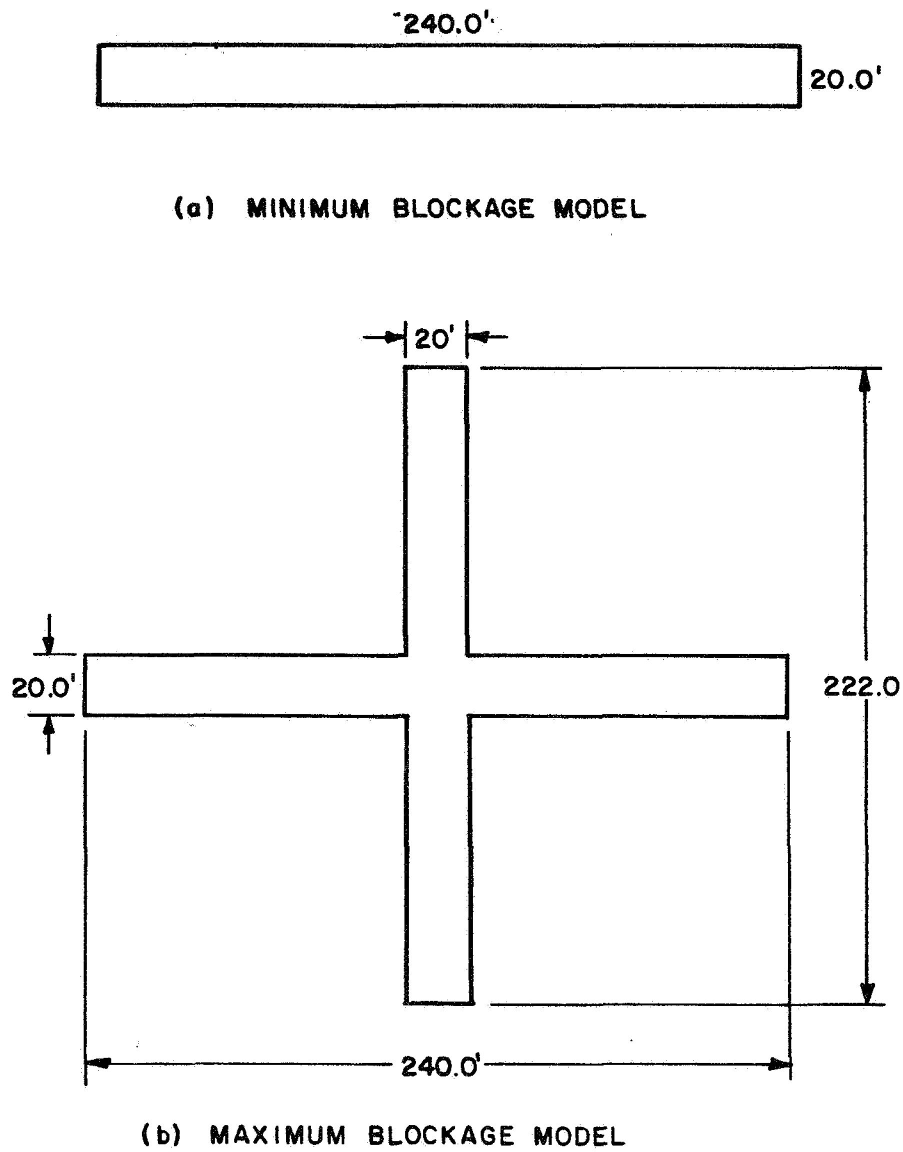


Figure 23. Simplified blockage model.

50272-101

| REPORT DOCUMENTATION PAGE | 1. REPORT NO. | 2. | 3. Recipient's Accession No. |
|---|---|---|---|

| | |
|---|---|
| 4. Title and Subtitle<br>SIMULATION OF AN AIRCRAFT FLYING THROUGH A GROUND STATION TO SATELLITE LINK | 5. Report Date<br>February 1986 |
| | 6. |
| 7. Author(s)<br>R.C. Rudduck, W.D. Burnside, A.K. Dominek, T.H. Lee | 8. Performing Organization Rept. No.<br>716148-7 |
| 9. Performing Organization Name and Address<br>The Ohio State University<br>ElectroScience Laboratory<br>1320 Kinnear Road<br>Columbus, Ohio 43212 | 10. Project/Task/Work Unit No. |
| | 11. Contract(C) or Grant(G) No.<br>(C)<br>(G) NSG 1613 |
| 12. Sponsoring Organization Name and Address<br>National Aeronautics and Space Administration<br>Langley Research Center<br>Hampton, Virginia 23665 | 13. Type of Report & Period Covered<br>Technical |
| | 14. |

15. Supplementary Notes

16. Abstract (Limit: 200 words)


The effect of an aircraft which flies through a ground station-to-satellite link is determined. There are two aspects to the work reported here: (1) an aperture blockage theoretical solution developed by Rudduck and Lee was used to calculate the effect of a large aircraft (C5) for various satellite ground station antenna diameters, and (2) the compact range facility at the Ohio State University was used to measure various targets, including a 737 aircraft, and to validate the theoretical solution in item (1).


17. Document Analysis a. Descriptors

b. Identifiers/Open-Ended Terms

c. COSATI Field/Group

| 18. Availability Statement | 19. Security Class (This Report)<br>Unclassified | 21. No. of Pages<br>45 |
|---|---|---|
| | 20. Security Class (This Page)<br>Unclassified | 22. Price |

(See ANSI–Z39.18) See Instructions on Reverse OPTIONAL FORM 272 (4–77) (Formerly NTIS–35) Department of Commerce